

Disclaimer/Publisher's Note: The statements, opinions, and data contained in all publications are solely those of the individual author(s) and contributor(s) and not of MDPI and/or the editor(s). MDPI and/or the editor(s) disclaim responsibility for any injury to people or property resulting from any ideas, methods, instructions, or products referred to in the content.

Review

# Transparent Self-cleaning Coatings: A Review

Pengyuan Wu <sup>1</sup>, Zhuanzhuan Xue <sup>1</sup>, Tianxiang Yu <sup>1</sup>, and Oleksiy V. Penkov <sup>1,2\*</sup>

<sup>1</sup> ZJU-UIUC Institute, International Campus, Zhejiang University, Haining, 314400, China

<sup>2</sup> Department of Mechanical Science and Engineering, University of Illinois Urbana-Champaign, Urbana, IL 61801, USA

\* Correspondence: oleksiypenkov@intl.zju.edu.cn

**Abstract:** Advanced coatings are essential to modern technologies, as they optimise surface characteristics for different application scenarios. Transparent and self-cleaning coatings are increasingly used as protective coatings for various applications, such as foldable touchscreens, windows, and solar panels. Moreover, incorporating other functionalities such as high hardness, wear resistance, and flexibility into transparent and self-cleaning coatings is important for broadening the use cases. Although many kinds of multifunctional coatings have been developed, it is still difficult to embody several properties in one coating adequately, as some properties, such as hardness and flexibility, are inherently contrastive. This review first describes basic principles, including wettability, photocatalytic reactions, photo-induced hydrophilic phenomena, and the implication of self-cleaning. The desired properties of multifunctional coatings are then listed, and methods for evaluating different properties are used. Recent progress in various preparation methods for multifunctional coatings, including the sol-gel, dip/spin, and chemical vapour deposition (CVD) methods, are also presented. Magnetron sputtering (MS) technology is widely used in coating preparation. Compared with chemosynthesis and CVD, MS is time-saving, suitable for industrial production, and environmentally friendly. Coatings prepared by MS usually possess excellent mechanical properties. Thus, we highlight the current research status of MS technology in multifunctional coating preparation. Moreover, according to the multilayer design structure of coatings, their optical and mechanical properties and self-cleaning ability can be controlled by combining the characteristics of different materials. Finally, combining photocatalytic materials such as TiO<sub>2</sub> with other materials through a multilayer structure to obtain a multifunctional coating with excellent overall properties is discussed.

**Keywords:** self-cleaning coatings; wettability; durability; mechanical properties; optical properties; photocatalysis; prepare methods

## 1. Introduction

Advanced multifunctional coatings are essential for modern technology, as coatings can modify the surface properties of different materials [1]. Among the various coatings, transparent and self-cleaning protective coatings have played a crucial role in several applications, such as automobile windshields, camera lenses, and wearable and foldable electronics in particular, as this field of applications has grown tremendously. Self-cleaning coatings are currently divided into two categories: hydrophobic [2,3] and hydrophilic [4,5]. These two kinds of coatings clean themselves through different water behaviours on their surface: sliding water for the former and sheeting water for the latter, both of which remove dirt [6]. Excellent mechanical properties are essential for practical application, regardless of the self-cleaning mechanisms. High hardness is needed to protect the coating against scratches [1], and wear resistance is crucial for maintaining a roughness-induced hydrophobic surface [7] and a super-hydrophobic structure [8].

Currently, it is easy to meet any one of the requirements for hardness, flexibility, wear resistance, transparency, or self-cleaning. However, combining such properties in one coating is still a formidable task, not to mention that high hardness and high flexibility are widely considered to be mutually exclusive [9]. Early inorganic glassy coatings are hard,



and they possess wear resistance [10,11], but their innately low toughness makes them easy to crack and shatter under long-term bending stresses [12]. At present, considerable effort is being made to achieve this goal. For instance, several organic materials having excellent flexibility and high transparency have been reported as protective coatings for foldable electronics [13–15]. However, because of their organic nature, most of them suffer from a low hardness of less than 1 GPa, even though it is difficult to protect the substrate from sand, which is composed of silica (hardness of silica is around 7 GPa) primarily. Moreover, their thermal stability, impact, and wear resistance are also low. These imperfections preclude the use of coatings in many applications. Organic-inorganic (O-I) hybrid materials developed using sol-gel chemistry [16–19] are fabricated as a common strategy for improving overall performance. Such coatings are fabricated from various precursors like silicone, metallic oxide, or alkoxides [16,20–22]. Inorganic and organic components provide appropriate hardness and flexibility to these systems, respectively. However, the hardness of O-I coatings is still much lower than that of ceramics or metals. Meanwhile, complex and time-consuming production processes are not conducive to mass production.

In addition to chemosynthesis, magnetron sputtering (MS) is also widely used to prepare coatings, and it allows the production of coatings having a wide range of properties [23]. For example, the hardness of coatings prepared by MS can range from 1 GPa to more than 45 GPa [24,25]. Moreover, the wettability of coatings can also be adjusted from super-hydrophilic [26–29] to super-hydrophobic [30–33]]; both of these different wettability values are serviceable for self-cleaning coatings in different surroundings [34,35]. Further, various properties of different materials can be combined in a multilayer structure [36]. These advantages make MS a promising candidate for the fabrication of durable self-cleaning coatings. However, there are still some trade-offs for both hydrophilic and hydrophobic MS-made coatings. For example, roughness and surface topography are essential for super-hydrophobic surfaces, but high roughness also reduces wear resistance [37] and sometimes reduces optical transparency [38,39].

Research and review papers that focus on the preparation, properties, and applications of self-cleaning coatings are increasing in number yearly. However, only some reviews focus on MS technology for self-cleaning coatings. This review briefly introduces the basic theory of wetting ability and how it relates to self-cleaning properties. Moreover, recent advances in multifunctional self-cleaning coatings are presented, with particular emphasis on methods for evaluating desired properties, including mechanical, optical, and self-cleaning properties. Multifunctional coatings prepared by MS technology and multilayer structure coatings will then be detailed.

## 2. Basic Theories of Wetting Ability and Self-cleaning Coatings

### 2.1 Basic Theories of Wetting Ability

Wetting ability is determined by the structure and chemical properties of surfaces [40]. Water contact angle (WCA) is usually the quantitative criterion for water-wetting ability. Surfaces can be classified by their WCA: 0°–10° means super hydrophilic, 10°–90° means hydrophilic, 90°–150° means hydrophobic, and when its WCA is larger than 150°, a surface is super-hydrophobic [40]. When a solid surface is tilted to the minimum angle at which water droplets roll down the surface, this minimum angle is called the sliding angle (SA) [41] or rolling angle (RA) [42]. For an ideal smooth, solid surface, the contact angle (CA) of any liquid can be calculated by an equation that was first proposed by Thomas Young [43]:

$$\cos \theta = (\gamma_{sv} - \gamma_{sl}) / \gamma_{lv} \quad (1)$$

In this equation,  $\theta$  means CA in equilibrium on the solid surface. It is called Young's CA and is shown in Figure 1a.  $\gamma_{sv}$ ,  $\gamma_{sl}$ , and  $\gamma_{lv}$  refer to the interfacial tension or surface energy of solid-gas, solid-liquid, and liquid-gas, respectively.

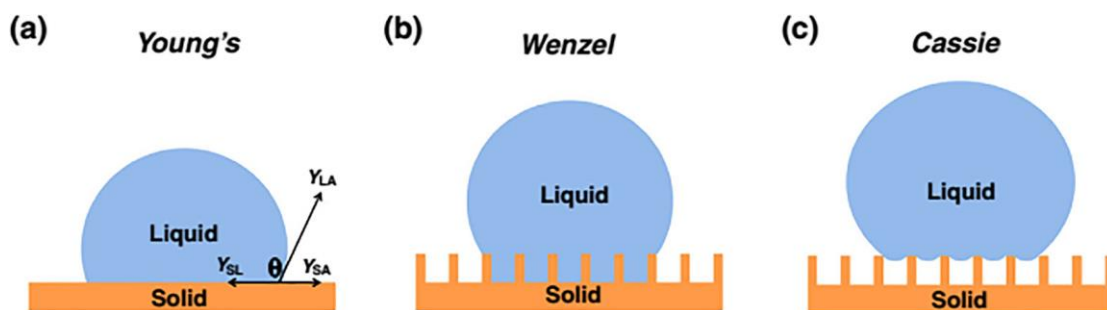


**Figure 1.** Wetting states: (a) Young; (b) Wenzel; (c) Cassie models. Reprinted with permission from *Journal of Coatings Technology and Research* [44]; Copyright 2015 Springer Nature

However, all surfaces in nature possess a certain roughness. Thus, the actual CA usually cannot be explained by Young's equation. For a better explanation of the wetting on rough surfaces, Wenzel and Cassie improved on Young's equation around the 1940s [45]. In Wenzel's model, a roughness factor ( $r$ ) was introduced as a modification to Young's model. Wenzel's model is shown in Eq. (2).

$$\cos \theta_w = r \cdot \cos \theta, \quad (2)$$

In this equation,  $\theta_w$  is the apparent CA (Wenzel's CA),  $r$  is the roughness factor, which is defined as the ratio of the actual solid-liquid contact area to the projected contact area (as shown in Figure 1b), and  $\theta$  is the intrinsic CA on a smooth surface (Young's CA). Later, Cassie and Baxter [45] refined the Wenzel model to fit some super-hydrophobic phenomena in nature, which the former model could not interpret. In Cassie's model, area fraction ( $f$ ) was introduced. If the wetting happened in a liquid-solid-vapour system, as shown in Figure 1c, the Cassie equation could be implemented as below [40,46]:

$$\cos \theta_c = f(\cos \theta + 1) - 1 \quad (3)$$

where  $f$  represents the proportion of solid-liquid contact area to the total contact area (solid-liquid and vapour-liquid),  $\theta$  means Young's CA, and  $\theta_c$  means Cassie's CA.

In summary, when a surface is intrinsically hydrophilic, the greater its surface roughness, the more hydrophilic it will be. When a surface is intrinsically hydrophobic, the rougher it is, or the smaller the contact area at its solid-liquid interface, the better its hydrophobicity.

## 2.2. Hydrophobic Self-Cleaning Surface

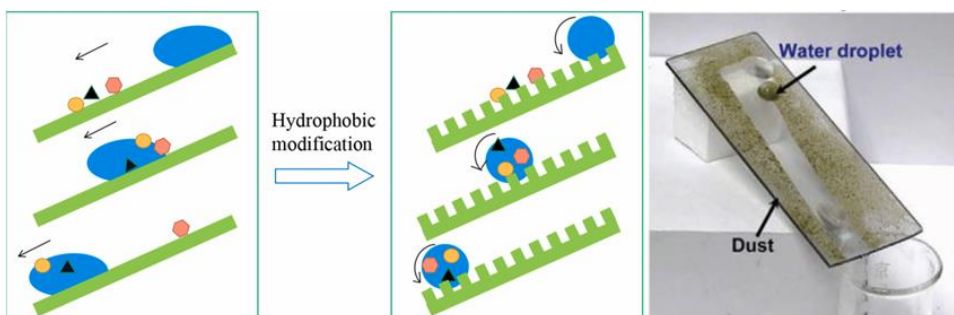


**Figure 2.** Diagram (Reprinted with permission from *Composites Part B: Engineering* [47]; Copyright 2022 Elsevier); and photograph (Reprinted with permission from *Advanced Materials* [48]; Copyright 2022 John Wiley and Sons) of the self-cleaning process

Hydrophobic surfaces have little or no tendency to absorb water molecules, which causes any surface water to form droplets and minimises the liquid-solid surface interface [49]. When the surface is tilted beyond the SA of the water droplet, the droplet rolls over the surface, picking up dust and moving it away from the surface [50], as shown in Figure 2. Generally speaking, water droplets cannot efficiently capture dust on a normal hydrophobic surface due to the non-slip boundary condition [51]. In the case of a hydrophobic rough surface that is super-hydrophobic, a lesser solid-liquid interface produces lower friction, and rolling droplets can carry contaminants away. The lotus leaf is the best-known example of this principle [52]. It does not mean, however, that greater roughness of a hydrophobic surface is preferable. Neither natural roughness-induced super-hydrophobic surfaces nor their artificial counterparts have good mechanical stability [53]. Thus, they cannot be used productively in harsh, heavily abrasive applications [37]. Moreover, a rough surface may also decrease optical transparency [39,54], which hinders its application in windshields, windows, and solar cells [55]. In some cases, even though the CAs and SAs of coatings do not qualify them as super-hydrophobic coatings, the coatings can still be called self-cleaning coatings [50,56], especially when excellent mechanical and optical properties are demonstrated.

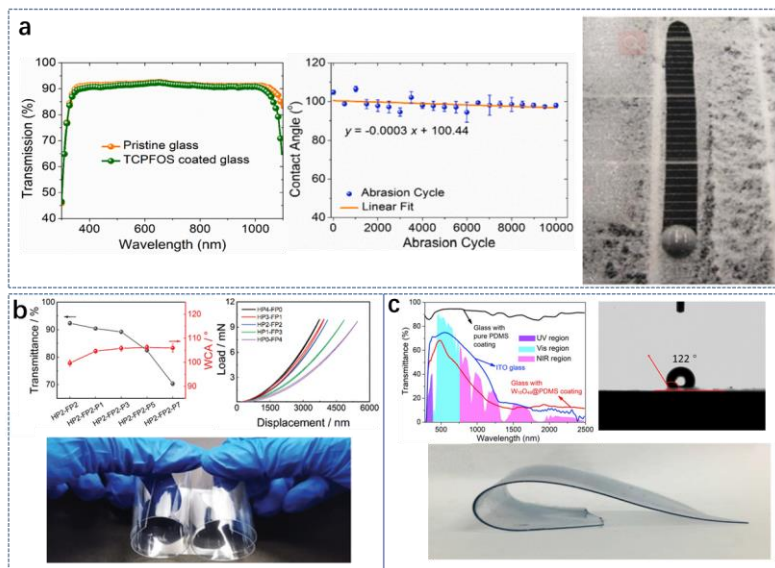


**Figure 3.** Normal hydrophobic coatings combine with special properties including high transparency, wear resistance, hardness and flexibility can be described as self-cleaning coatings. (a) Reprinted with permission from *Materials Chemistry and Physics* [57]; Copyright 2020 Elsevier. (b) Reprinted with permission from *Advanced Science* [50]; Copyright 2022 John Wiley and Sons. (c) Reprinted with permission from *Ceramics International* [58]; Copyright 2020 Elsevier.

### 2.3. Hydrophilic Self-cleaning Coatings

Hydrophilic coatings exhibit several desirable characteristics, particularly pertaining to their self-cleaning capabilities. Due to the hydrophilic nature of these coatings, water spreads on their surface and picks up soil [59]. Moreover, hydrophobic contaminants such as oil either cannot adhere to a hydrophilic surface or are easily removed through washing [4,60]. In addition to having self-cleaning properties, hydrophilic surfaces are also important to the fabrication of transparent devices, as the water droplets tend to spread and interconnect with each other to form a film that prevents the formation of fog [61]. A schematic of the self-cleaning mechanism is shown in Figure 4.

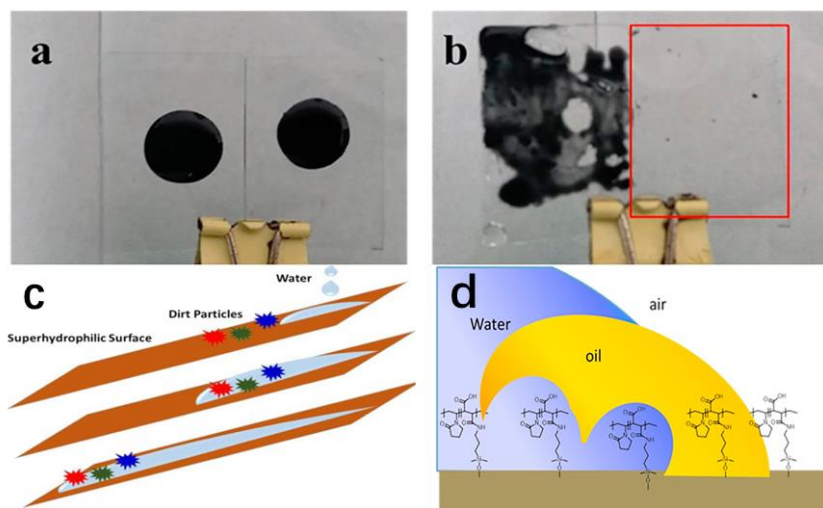


**Figure 4.** (a) and (b), self-cleaning property of the bare glass(left) and glass modified by hydrophilic coating(right) before and after washing with water. The contamination was mixed with silicone oil and activated carbon. Reprinted with permission from *Chemical Engineering Journal* [4]; Copyright 2018 Elsevier. (c-d), schematic of hydrophilic self-cleaning mechanism for soil (Reprinted with permission from *Solar Energy* [59]; Copyright 2020 Elsevier) and oil (Reprinted with permission from *Chemical Engineering Journal* [4]; Copyright 2018 Elsevier).

Hydrophilic self-cleaning is often based on photocatalysis and photo-induced super hydrophilicity [62–64], which allow self-cleaning coatings to clean themselves and their environment. For photocatalysis materials such as  $\text{TiO}_2$  [65], if the light energy is higher than the band-gap energy of  $\text{TiO}_2$ , an electron can be excited from the valence band to the conduction band, which then generates a hole in the valence band. If the charge carriers can escape the charge-annihilation reaction and migrate to the surface, the photoexcited electrons can reduce atmospheric  $\text{O}_2$  to generate superoxide radicals( $\bullet\text{O}_2^-$ ) or hydroperoxyl radicals( $\text{HO}_2\bullet$ ). The valence band hole can oxidise surface-adsorbed water or  $\text{OH}^-$  to produce  $\bullet\text{OH}$ . These reactive oxygen species can convert organic pollutants into  $\text{CO}_2$  and water, which cleans the surface. There are different explanations for the mechanism of photo-induced hydrophilicity. The mechanism that relies on the formation of surface defects upon UV light illumination was first explained by Wang et al. [66,67] and is already widely accepted. The observation is that exposure to UV light can transform  $\text{TiO}_2$  surfaces from hydrophobic to significantly amphiphilic. This change is attributed to the creation of  $\text{Ti}^{3+}$  defect sites by the photogenerated process, which promotes the dissociative adsorption of water molecules.

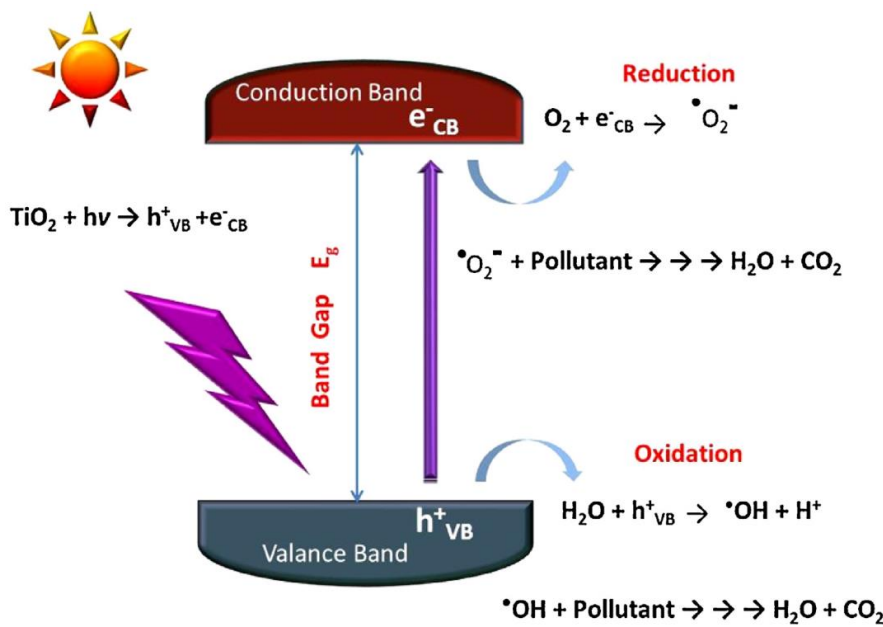


**Figure 5.** Schematic illustration of photocatalysis and photo-induced super hydrophilicity. Reprinted with permission from *Applied Catalysis B: Environmental* [65]; Copyright 2015 Elsevier.

### 3. Desired Performance of Transparent Self-cleaning Coatings and Measurement Methods

#### 3.1. Mechanical Performance

##### 3.1.1. Hardness and Flexibility

Coatings with hardness and flexibility are essential in many applications, such as flexible electronics [68], micro-electro-mechanical systems [69], and the deposition on flexible substrates such as polymers [2]. Hard and flexible coatings are defined by Musil [70] as having: a relatively low effective Young's modulus  $E^*$  that has a high ratio with hardness ( $H/E^* \geq 0.1$ ); high elastic recovery  $W_e \geq 60\%$ ; a dense, void-free microstructure. Foldable smartphones, wearable electronics, and OLED-based televisions are anticipated to feature flexible displays [71]. All the applications require protective coatings that are transparent and self-cleaning but also flexible and hard to prevent scratches and dents. In addition, high hardness is required to improve the stability of super-hydrophobic structures [72]. As mentioned in the first section, the flexibility of polymer coatings prepared by sol-gel methods is pretty, but the hardness is usually less than 1 GPa. Inorganic coatings that are prepared by physical methods such as MS technology can easily obtain high hardness, but it is difficult for them to obtain a high value of  $H/E$ .

Nanoindentation tests and pencil hardness tests are the main methods for evaluating the hardness of coatings. The latter is often used to test the hardness of polymer coatings. The largest value of pencil hardness is 9H, which is approximately equal to 0.52~0.75 GPa of Martens hardness, which is obtained from nanoindentation tests [71]. Flexibility can also be evaluated by the value of  $H/E$  obtained from nanoindentation tests. Moreover, the bending test is an intuitive approach to measuring flexibility. Different test types exist, such as the static test method described in GB/T 1371-93, this method requires the relevant test equipment [50]. Furthermore, the dynamic bending test is performed on a continuous bending apparatus [1]. These two test methods are shown in Figure 6.



**Figure 6.** (a) Flexibility tester [73], coatings were deposited on tinplate and bent on shaft rods of different diameters in this method. The flexibility was determined by the minimum diameter of the shaft rod that did not make the coating crack after bending [50]. (b) Photograph of the dynamic bending test. Reprinted with permission from *Composites Part B: Engineering* [13]; Copyright 2022 Elsevier.

### 3.1.1. Mechanical Durability

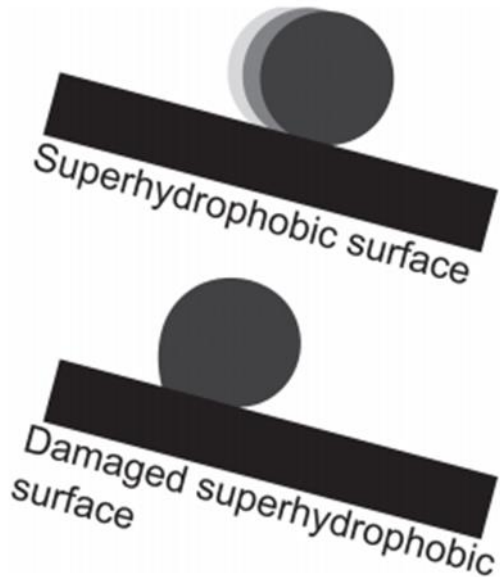


**Figure 7.** Damaged super-hydrophobic surface showing higher contact angle hysteresis, which leads to droplets sticking to the surface. Reprinted with permission from *Advanced Materials* [53]; Copyright 2010 John Wiley and Sons.

In addition to the bending property related to the flexibility of coatings, research on mechanical durability, including wear and abrasion resistance, has mainly been done on super hydrophobic self-cleaning coatings, as their self-cleaning ability and non-wetting ability rely on a flimsy surface structure. The super-hydrophobicity of a structured surface can be reduced mainly in two ways [53]: (a) the area of contact between the water and the surface increases due to a loss of roughness, and (b) the hydrophobic surface layer is destroyed, which results in the exposure of the intrinsically hydrophilic inner layer material. The difference in the behaviour of water droplets before and after the destruction of the super-hydrophobic surface is shown in Figure 7. In addition to improving a coating's intrinsic hardness and wear resistance, many efforts have been made to enhance its mechan-

ical durability. Hierarchical roughness, which contains nano/micro length scales, can increase the mechanical stability of the super-hydrophobic surface structure [74,75]. The basic concept of hierarchical roughness involves using robust microscale structures to provide spatial protection for relatively fragile nanoscale protrusions from mechanical damage, which enhances surface roughness and non-wettability, as shown in Figure 8. Moreover, fabricating self-healing structures [76,77] can also enhance the mechanical durability of hydrophobic self-cleaning coatings.

The methods used to evaluate mechanical durability include scratch-resistant testing and wear testing. The scratch resistance testing is usually performed using a hard abrasive tip [50,78] (the hardness of the tip depends on the hardness of the coatings) and scratching the coating under a certain load to compare the changes in the scratch tracks and the transmission of light, etc. The abrasion test involves the circular sanding of the coating under a certain load using steel wool [50], sandpaper [79], and so on. Afterward, the scratches, wear rate, surface structure, and changes in properties are analysed. The scratch and wear tracks are shown in Figure 9.

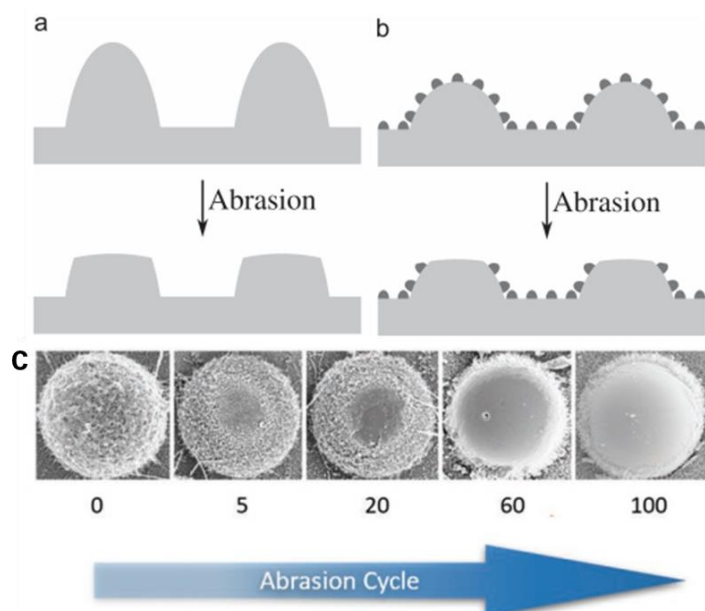


**Figure 8.** (a-b) schematic of the production effect of microscale structure to nanostructure [53]. Reprinted with permission from *Advanced Materials* [53]; Copyright 2010 John Wiley and Sons. (c) SEM images of hierarchical roughness with incremental abrasion cycles. Reprinted with permission from *Small* [75]; Copyright 2019 John Wiley and Sons.

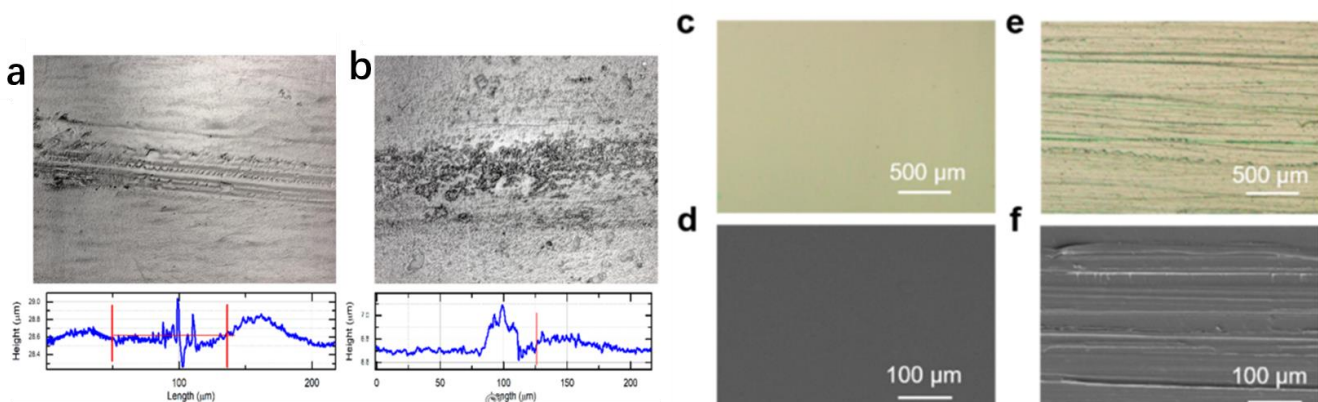


**Figure 9.** (a) Scratch tracks in PET, (b) PET substrate with Si<sub>x</sub>N<sub>x</sub>/BN coatings. Si<sub>3</sub>N<sub>4</sub> ball was used as tip and a normal load of 50 mN was applied. Reprinted with permission from *ACS Applied Materials*

*& Interfaces* [78]; Copyright 2019 American Chemical Society. (c) and (e) Optical micrographs of polymer coating before and after wearing. (d) and (f) SEM micrographs of polymer coating before and after wearing. Reprinted with permission from *Applied Materials* [1]; Copyright 2022 American Chemical Society.

### 2.1.3 Adhesion to Substrate

Adhesion strength is essential, especially for flexible coatings [37], as it represents the coating's resistance to separation from the substrate when vertical tension is applied [80]. For coatings prepared by sol-gel methods, weak adhesion between the coating and the substrate sometimes presents barriers to their practical application [81]. Many efforts have been made to improve the adhesion strength of coatings. For example, introducing polar groups on the surface allows inter- and intramolecular hydrogen bond formation, which results in better substrate adhesion performance [80]. However, this method may make the coating more likely to attract dust, and it is unsuitable for hydrophobic self-cleaning coatings. In order to make super-hydrophobic surfaces that have high substrate adhesion, Zhang introduced donor-acceptor self-assembly to nanoparticles having a polyurethane matrix and metal-organic framework [82]. In this report, the enhancement of adhesion strength was due to aromatic group stacking during donor-acceptor self-assembly [83]. In addition to the chemical preparation methods, many strategies have been developed to improve the adhesion strength of physically made coatings. Sun [81] used oxygen plasma to modify a polycarbonate substrate to enhance adhesion and then deposited  $\text{SiO}_2/\text{TiO}_2$  films on the substrate using pulsed laser deposition. Because different substrates and coatings have different properties, we should select specific methods to obtain the desired adhesion strength.

There are different ways to test adhesion strength, such as the tape test, pull-off test, shear lap test, three- and four-point bending test, and the crosshatch test. A detailed description of these test methods can be found in research published by Rezaee [84]. Moreover, the schematics of these methods can be viewed in Figure 10.

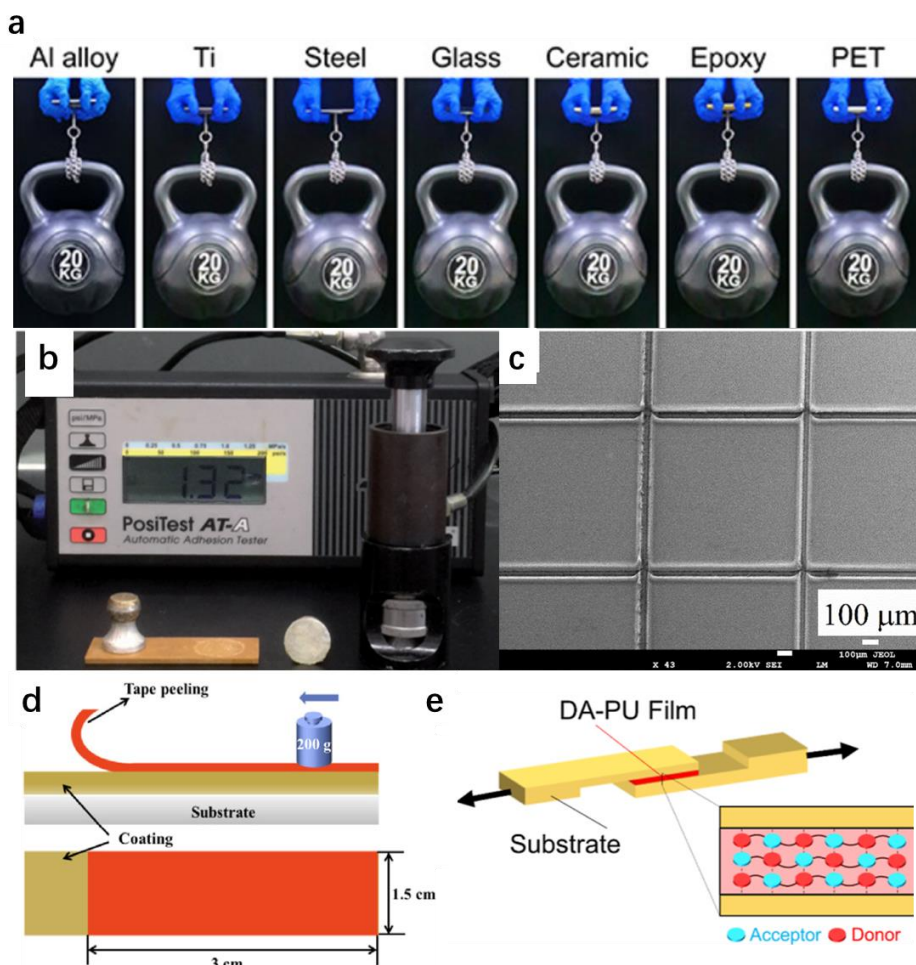


**Figure 10.** Schematics of different methods of testing for adhesion strength: (a) pull-off method. Reprinted with permission from *Applied Materials* [80]; Copyright 2023 American Chemical Society. (b) Tester for pull-off method. Reprinted with permission from *Journal of Materials Chemistry. A* [15]; Copyright 2020 Royal Society of Chemistry. (c) Crosshatch test method. Reprinted with permission from *Applied Surface Science* [81]; Copyright 2022 Elsevier. (d) Tape test method. Reprinted with permission from *Friction* [35]; Copyright 2023 Springer Nature. (e) Shear lap test method. Reprinted with permission from *ACS Applied Materials & Interfaces* [82]; Copyright 2023 American Chemical Society.

## 2.2. Optical and Self-cleaning Properties

### 2.2.1. Optical Properties

Optical properties include transmittance, reflectance, and absorptivity. The testing method for optical properties is relatively fixed. A spectrophotometer can obtain all the spectrums [50,78,85]. When a beam of light strikes any object, the light will be reflected, absorbed, or transmitted. Hence, to improve transmission, reflection and absorption must be reduced, as per the following equation [86]:

$$\alpha + \rho + \tau = 1 \quad (4)$$

where  $\alpha$ ,  $\rho$ , and  $\tau$  mean absorptivity, reflectivity, and transmissivity, respectively. Because it is a relatively easy task to reduce absorptivity through modern means of material synthesis, the common strategy for enhancing transmission is to decrease reflectivity with antireflective (AR) coatings [86], including interference layers [86] and inhomogeneous layers or surface structures [87]. Inhomogeneous layers and surface structures call for a compromise between optical and mechanical properties [88], so it is not preferred.

Currently, there are three main strategies for designing AR coatings [49]: design quarter-wave single-layer, graded-index coating, and multilayer interference coating (shown in Figure 11). For the first method, the optical thickness of the coating should be  $\lambda/4$ , and the refractive index of the coating ( $n_c$ ), substrate ( $n_s$ ), and air ( $n_{air}$ , equal to 1) should conform to the following equation [49]:

$$n_c = (n_{air} n_s)^{1/2} \quad (5)$$

Single-layer coatings eliminate reflection only at a specific wavelength, which hinders their application in areas where broadband AR characteristics are a prerequisite. The second method relies on gradually decreasing the refractive index of coatings, from the value of substrate (high refractive index) to the value of air (low refractive index). The general tool for achieving this goal is building moth-eye nanostructures or controlling nanoporosity throughout a coating [89]. However, this method is hindered by poor mechanical properties, as mentioned. The third type of AR coating comprises a series of layers with varying thicknesses, which alternate between high and low refractive indexes [90]. By appropriately arranging different uniform layers, it is possible to optimise the destructive interference of reflected light at various interfaces, thereby minimising the overall reflection of light. This method offers a significant advantage, as it enables the AR capability to extend across a wide range of incident angles and a broad spectrum of wavelengths, which encompass the UV range to the near-IR range.

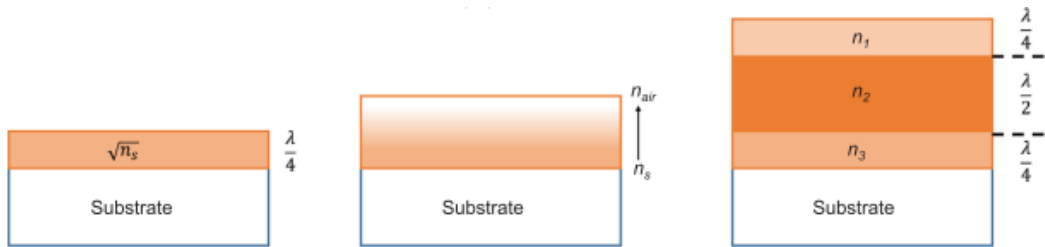


**Figure 11.** Three main design strategies for AR coatings: quarter-wave single-layer coating, graded-index coating, and multilayer interference coating. Shear lap test method. Reprinted with permission from *Applied Energy* [49]; Copyright 2020 Elsevier.

## 2.2.2 Self-cleaning Properties of Hydrophobic Coatings

Measuring the WCA and SA of hydrophobic coatings can initially determine whether the coating performs self-cleaning. If the WCA of the coating is greater than  $150^\circ$  and the SA is less than  $10^\circ$ , this coating is likely to have good self-cleaning properties [6]. In some cases, researchers conduct simulated contamination experiments on coatings. If the contaminated coating can easily be cleaned, even if its CA and SA data are less than ideal, it can be called a self-cleaning coating [50,57]. Contamination-cleaning experiments typically use contaminants such as dust, dirt, or carbon particles to soil the coating and then add droplets to the coating to see whether the droplets carry the contaminants off the coating surface, as shown in Figure 2. Using this kind of method to evaluate self-cleaning performance is relatively subjective. A method that used spectrophotometric measurement to test the self-cleaning efficiency of coatings was designed by Kumar et al. In this method [14,91], the lightness (L1) values of the as-prepared coatings were first measured using a spectrophotometer over five points spread uniformly across the sample surface. A 10-mL special artificial dirt solution was then sprayed over the test samples, and the samples were then mounted at an angle of  $45^\circ$  to the ground. The dirt was left to dry overnight and then heated at  $60^\circ\text{C}$  for an hour, as shown in Figure 12a. The drying step in this process is important because wet dirt can be thoroughly cleaned off all coatings. The lightness values were measured again after the dirt dried and were recorded as L2. Next, 10 mL of clean water was sprayed at a pressure of 3 bar from a distance of 25~30 cm over the samples mounted at the same angle, as shown in Figure 12b. The lightness values after cleaning were measured and recorded as L3, shown in Figure 12b. The amount of

dirt that had accumulated on the samples before and after the cleaning was calculated as  $[(L_1 - L_2)/L_1 \times 100]$  and  $[(L_1 - L_3)/L_1 \times 100]$ . The self-cleaning efficiency was defined as  $\left[100 - \left\{\frac{(L_1 - L_3)}{L_1} \times 100\right\}\right]$ .

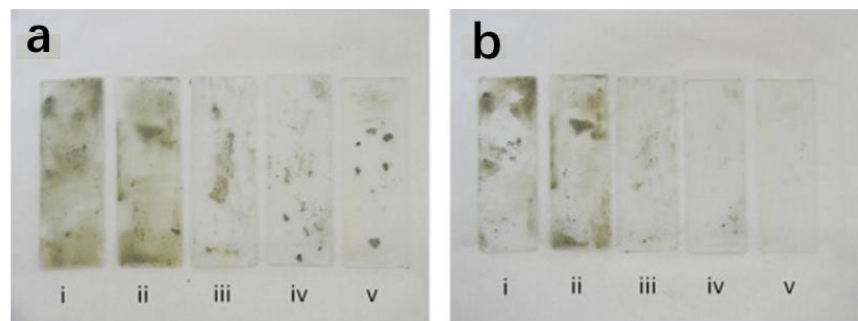


**Figure 12.** Photographs of (a) coatings after dirt spray and (b) coatings after water spray for cleaning. Reprinted with permission from *Applied Surface Science* [91]; Copyright 2015 Elsevier.

### 2.2.3 Self-cleaning and Photocatalytic Properties of Hydrophilic Coatings

Hydrophobic coatings can remain free from dirt and grime. Nevertheless, if a surface is ruined with oil contaminants, its self-cleaning capability will be lost due to its lipophilicity [60]. As we mentioned in Section 1.3, a hydrophilic surface is usually oleophobic, which can be used as another kind of self-cleaning surface. Water can wash away oil without detergent on this kind of surface. Furthermore, coatings that have photocatalytic properties may possess super hydrophilic properties and degrade surface organic pollutants through photocatalytic reactions [34]. CA measurements, photocatalytic efficiency testing, and contamination-cleaning testing are used to evaluate the performance of such coatings [34,64]. Photocatalytic efficiency testing includes two parts: the evolution of wetting properties and the degradation rate of organic pollutants under UV or visible light irradiation. The change in wettability can be obtained by measuring the curve of the WCA over time under certain illumination, as shown in Figure 13a. The degradation rate of the pollutant by the coating can be obtained by measuring with a spectrophotometer the change in the concentration of organic matter (such as methyl orange) in the solution under a certain amount of light, and the concentration equalling the photocatalytic activity is calculated using Equation (6) [92]:

$$\eta = \left[ \frac{C_0 - C_t}{C_0} \right] \times 100\% \quad (6)$$

The degradation of organic matter is also considered a first-order dynamic reaction, as shown in Equation (7) [92]:

$$-\ln \left( \frac{C_t}{C_0} \right) = kt \quad (7)$$

In these two equations,  $C_0$  is the initial concentration,  $C_t$  is the concentration at time  $t$  of irradiation, and  $k$  is the reaction rate. Figure 13b shows the relevant curves.

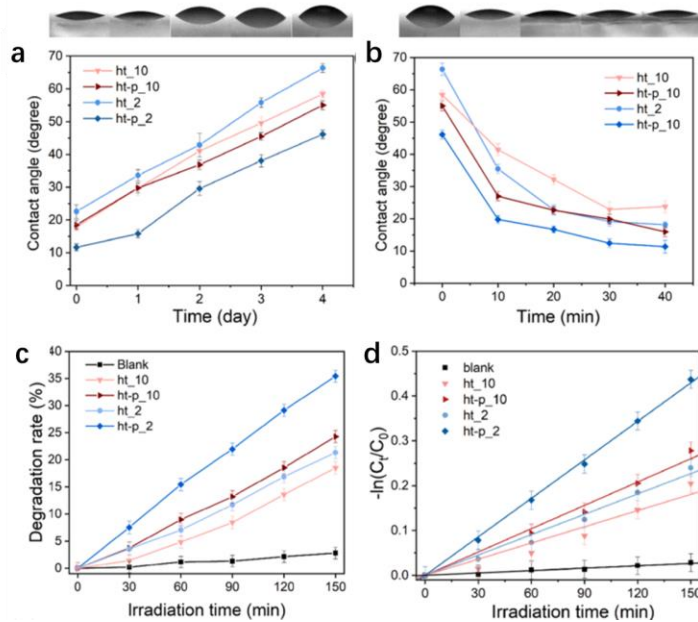


**Figure 13.** Process of WCA (a) increase and (b) decrease by the coatings under dark conditions and ultraviolet irradiation, respectively. (c) Photocatalytic degradation of methyl orange, and (d) degradation kinetics curves. Reprinted with permission from *Applied Surface Science* [92]; Copyright 2023 Elsevier.

#### 4. Fabrication Methods and Materials for Multifunctional Coatings

Some methods for the preparation of multifunctional coatings have already been mentioned. In this chapter, we detail some common preparation methods and the materials used for such coatings. In addition, their advantages, disadvantages, and applicability will also be discussed. The preparation process for hydrophobic coatings can generally be divided into two steps: construction of surface roughness and modification using low-surface-energy materials [93]. There are many ways to achieve such goals. For example, laser burning [94], surface etching [95], photolithography [52], and plasma treatment [96] can be used to create surface roughness. Moreover, materials having low surface energy, such as carbon fluoride [42], silicones [14], metal oxides and nitrides [55], can be used for surface treatment, used as fillers, or used to prepare coatings. For hydrophilic coatings,  $\text{SiO}_2$  [60],  $\text{TiO}_2$  [97], and rare earth oxides [34] are commonly used raw materials because of their special surface properties and band-gap energy. Considering the other optical and mechanical performance requirements, the available methods are limited. The most commonly used methods are introduced in this review and include the sol-gel method, dip/spin-coating [98], and the chemical vapour deposition (CVD) method.

##### 4.1. Coatings Deposited by Sol-gel Method Combined with Dip/spin Method

The sol-gel method is the most commonly used method for conventional coatings [59]. This process proceeds by converting a precursor mixture (such as a water or alcohol solution) into a homogeneous gel under certain conditions [99]. This method is useful for both hydrophobic and hydrophilic coatings. The application of this method is inexpensive, practical, and includes few technical details [59]. However, the deposition process of this method is difficult to control, so it usually needs spin and dip coating according to the process shown in Figure 14. Developing organic-inorganic hybrid coatings based on sol-gel chemistry is an effective way to obtain hard and flexible coatings [100]. Zhang et al. [50] reported a highly cross-linked multifunctional epoxy-siloxane hybrid coating by combining sol-gel chemistry with an epoxy-amine curing reaction. The reacted solution was then dropped on various substrates and dried. In their study, the resulting coating exhibited high transmittance under visible wavelength, ceramic-like hardness, and poly-

mer-like flexibility because of the unique combination of siloxane nanoclusters and polymer networks. Meanwhile, because the coating contained fouling-resistant telomers and the low surface tension liquid lubricant polydimethylsiloxane (PDMS), it exhibited excellent anti-biofouling and self-cleaning properties with a relatively small WCA. Yang et al. prepared hydrophilic silicon dioxide film on an acrylate polyurethane substrate using the sol-gel and spin methods.  $\text{SiO}_2$  and tetraethoxysilane served as precursors, and water and ammonium hydroxide as solvents in this process. The reacted sol was spin-coated onto the substrate and then dried. Finally, the coating showed a small WCA of  $16^\circ$ , with self-cleaning performance. If the inorganic material chosen for the organic-inorganic hybrid system is titanium dioxide, a coating can further enhance its functionality by degrading surface organic pollutants through photocatalytic reactions [101–103]. For example, Azam et al. [103] prepared transparent  $\text{TiO}_2$  and metal-doped  $\text{TiO}_2$  nanocrystalline films via an affordable and facile sol/gel dip-coating method to improve the self-cleaning performance of the glass covers of solar panels. The metal-doped  $\text{TiO}_2$  showed enhanced efficiency for methylene blue degradation.

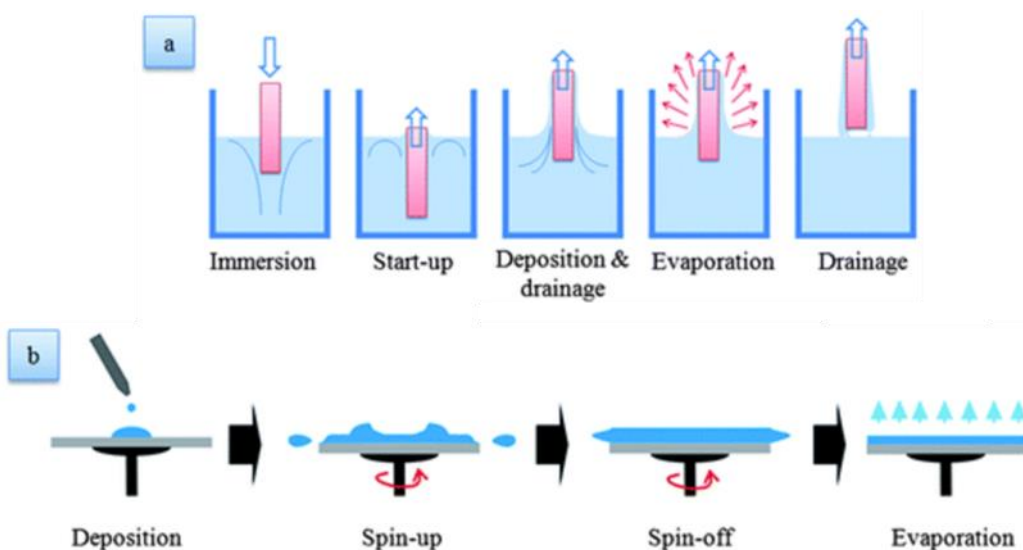


**Figure 14.** (a) Dip-coating and (b) spin-coating processes. Reprinted with permission from *Energy & Environmental Science* [104]; Copyright 2008 Royal Society of Chemistry.

#### 4.2 CVD Method

The CVD vacuum deposition method produces high-quality, high-performance solid materials. It is one of the most popular coating methods, like the sol-gel method. In a typical CVD process, the substrate is exposed to volatile precursors, which react and/or decompose on the substrate surface to produce the desired deposit [65]. This method is commonly used for optical purposes with glass applications, as a desired refractive index can be obtained [59]. Furthermore, the composition and structure of coatings can be easily controlled by the deposition conditions. Park et al. [105] reported a single-step aerosol-assisted CVD (AACVD) method in which Al-doped  $\text{ZnO}$  nanoparticles were functionalised in a mixture of PDMS, epoxy resin (EP), and steric acid (SA) and were used as a precursor. They obtained an EP/PDMS/SA/Al $\text{ZnO}$ -coated super-hydrophobic surface with good self-cleaning performance. Moreover, CVD techniques have been extensively researched for the deposition of  $\text{TiO}_2$  thin films on various substrates for self-cleaning and optical properties. Using an open-air liquid-assisted plasma-enhanced deposition process, Rodolphe et al. [106] deposited transparent amorphous  $\text{TiO}_2$  layers at atmospheric pressure. Lin et al. [107] prepared FTO/ $\text{TiO}_2$  tandem films using AACVD, followed by an annealing process. These coatings had a minimum CA of only  $5^\circ$ , indicating they were likely to exhibit good self-cleaning properties. CVD techniques can also be combined with other methods, such as sol-gel and template approaches, to obtain desirable properties. Zhang

et al. [108] reported a novel template for fabricating highly transparent, fluorine-free super-hydrophobic coatings. This research used PDMS as the silica source and multi-walled carbon nanotubes as the sacrificial template, followed by a CVD process to render the surface hydrophobic.

## 5. MS-made Multifunctional Coatings

MS is also a popular method to use in depositing thin films, as it has the advantages of a controllable film thickness, high purity, high deposition speed, favourable adhesion, easy operation, and environmental friendliness. [109] Utilising MS technology, it is possible to deposit a wide range of materials, provided that they can be prepared as magnetron targets. MS is technically divided into two types [40] according to different power sources, including direct current (DC) and radio frequency (RF) power sources. The DC-MS method is used to sputter conductive materials, and the RF-MS method is used to sputter non-conductive materials. The commercial application of self-cleaning titanium dioxide coatings prepared by MS technology has long been in use. Numerous studies have shown that utilising MS technology to design and prepare periodic layered nanostructures containing different materials effectively adjusts the hardness and flexibility of the coatings [36]. Furthermore, according to the different properties of the materials in the periodic multilayer nanostructures, the overall properties of the coatings can be flexibly adjusted [78], such as adhesion to the substrate, surface wettability, and electronic structure. Therefore, periodic multilayer nanostructures have great potential in multifunctional coating preparation. This chapter first introduces the conventional hydrophobic/hydrophilic multifunctional coatings prepared by MS technology and their potential applications in self-cleaning. Subsequently, the principles of periodic nano-multilayer structures and the relevant progress in multifunctional coatings based on this structure will be detailed.

### 5.1 MS-made Hydrophobic Multifunctional Coatings

As the MS method can deposit any kind of coating, intrinsically hydrophobic material can be used as the target in preparing hydrophobic coatings. Polytetrafluoroethylene (PTFE) is a commercial material that is highly prevalent in bulk and thin film forms owing to its exceptional corrosion and chemical resistance, outstanding thermal stability, exceedingly low surface energy, and insolubility in conventional solvents. Moreover, thin films of PTFE also exhibit a low refractive index of approximately 1.4 [110], which indicates its potential for optical applications. As early as 2010, Kim et al. [111] prepared super-hydrophobic PTFE coatings on an etched Al surface by the RF-MS method. The Al substrate was etched by 7 wt.% HCl solution for different durations to create different surface roughnesses. The PTFE film was then coated on this surface. As the thickness decreased, the CA gradually increased to 162°. Tripathi et al. [112] investigated the optical and microstructural properties of RF-MS sputtered PTFE films for hydrophobic applications. All the coatings showed high transmittance and hydrophobicity, which suggested their potential for self-cleaning multifunctional applications. However, the hardness and thermal stability were both low. Zenken et al. [113] discovered that the oxides and nitrides of numerous low-electronegativity metals exhibited inherent hydrophobic properties, coupled with exceptional mechanical properties such as high hardness levels of up to approximately 20 GPa and remarkable thermal stability exceeding 1000 °C. Figure 15 shows why this kind of surface is hydrophobic. Musil et al. [114] prepared flexible hydrophobic ZrN film by the DC-MS method, and the WCA of the film reached 93°. This film also showed a high hardness of 21.1 GPa, and its value of H/E was 0.125, which suggests it possesses good flexibility. Recently, a transparent and hydrophobic CeO<sub>2</sub> film with stable mechanical properties was presented by Zhu et al. [55]. The DC-MS method was used to deposit CeO<sub>2</sub> film on glass. According to the oxygen flow ratio adjustment, films having different surface roughnesses and surface chemical compositions were produced to achieve optimal transparency and mechanical properties. The max value of WCA reached 109.4° with a relatively low surface roughness (3.18 nm). Moreover, the deposition of CeO<sub>2</sub> films onto

glass substrates provided an optical transmittance of 84.0% at 550 nm. No mechanical damage or hydrophobicity loss was imposed on the films after the solid particle bombardment, tape peeling, and linear abrasion, as shown in Figure 16.

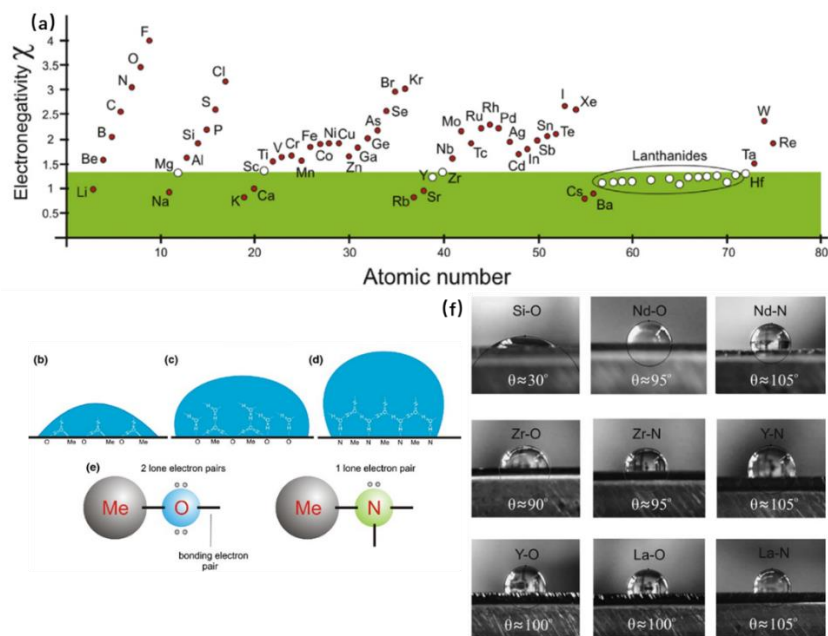


**Figure 15.** Characteristics that determine the hydrophilicity/hydrophobicity of material surfaces. (a) Graphical representation of Pauling electronegativity of elements. (b) Hydrophilicity of the surface of an oxide of a high-electronegativity metal. (c) Hydrophobicity of the surface of an oxide of a low-electronegativity metal. (d) Increased hydrophobicity of the surface of a nitride of a low-electronegativity metal compared with the corresponding oxide. (e) Schematic of bonding an oxygen or nitrogen anion to a metal cation in the film. (f) Measurements of the WCA of various surfaces. Reprinted with permission from *Journal of the American Ceramic Society* [113]; Copyright 2014 John Wiley and Sons.

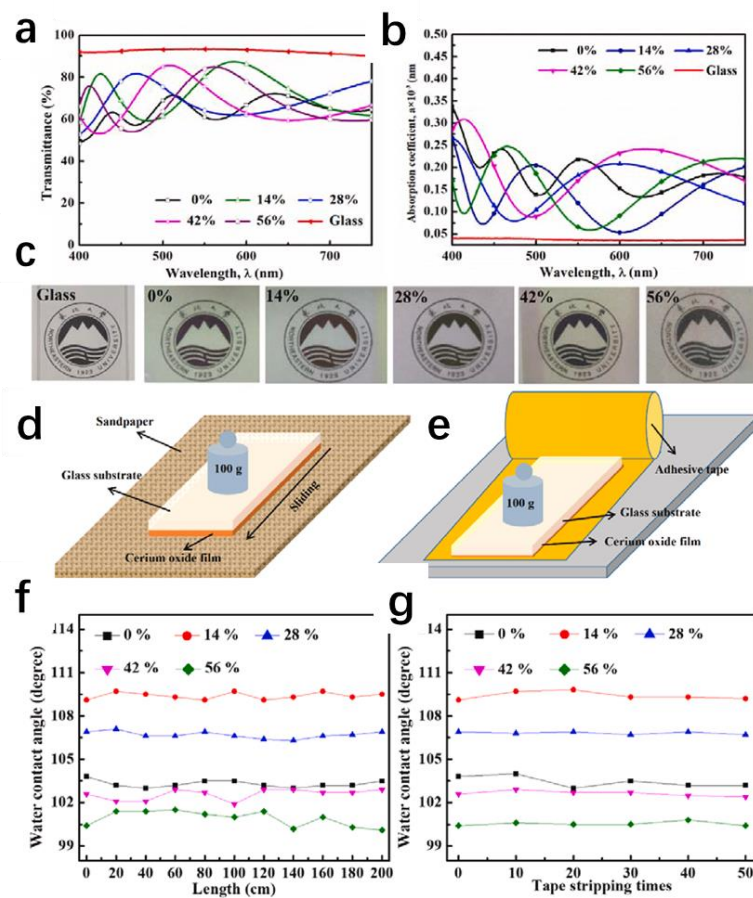


**Figure 16.** (a)-(c) Transmittance, absorption spectrum, and photo pictures of films with different O<sub>2</sub> flow ratios. (d), (e) Linear abrasion and peeling test. (f), (g) Plots of mechanical abrasion and peeling cycles as a function of WCA. Reprinted with permission from *Vacuum* [55]; Copyright 2021 Elsevier.

The WCA of smooth hydrophobic surfaces is unlikely to exceed 120° [44], which is generally insufficient for self-cleaning coatings. To improve the hydrophobicity of a coating, it is necessary to increase its surface roughness. The MS method allows for control of the surface morphology of the coating through the adjustment of the deposition parameters, as shown in Figure 17. However, as we all know, if the internal grain size is coarse and the structure is loose, the coating will not have good mechanical properties. It will not meet the requirements for a flexible hard coating with a 'dense, void-free microstructure' as we described. It is difficult to prepare coatings with super-hydrophobic surfaces using the MS method. Though the MS method can be combined with other methods in the preparation of a structured surface, it is still difficult to avoid the influences of high roughness on wear resistance and optical properties.

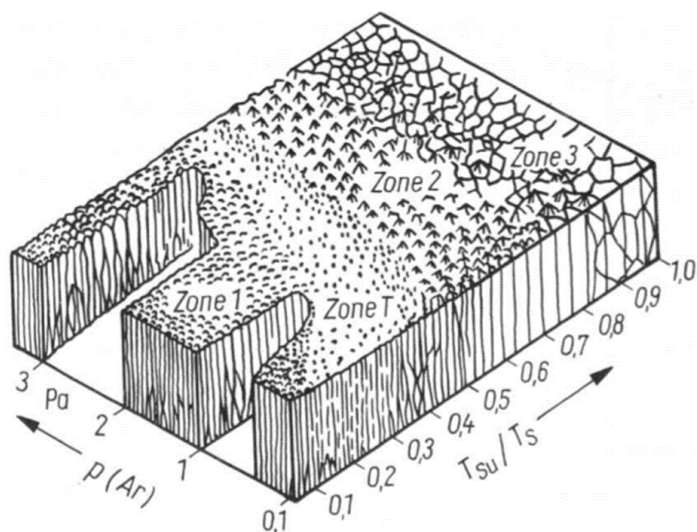


**Figure 17.** Schematic representation of the influence of substrate temperature and argon pressure on the microstructure of metal coatings deposited using cylindrical MS sources.  $T$  (K) is the substrate temperature, and  $T_m$  (K) is the melting point of the coating material. Reprinted with permission from *Materials Science and Engineering: A* [115]; Copyright 2003 Elsevier.

### 5.2 MS-made Photocatalytic Multifunctional Coatings

In order to make the self-cleaning function more efficient, the composition of such coatings often contains semiconductor materials with photocatalytic properties, such as  $TiO_2$  [97],  $CeO_2$  [34], and  $Cu_xO$  [85].  $TiO_2$  is one of the most famous photo-activated materials. Owing to its high photocatalytic efficiency, chemical stability, relatively low cost [116], wide transparent region (approximately 350–1200 nm [117]), and refractive index close to that of glass (2.2–2.7 for  $TiO_2$  and 2.1–2.2 for glass) [117,118],  $TiO_2$  is suitable for use as a high refractive index layer in multilayer AR film with self-cleaning properties. A single-component but bilayer AR coating of  $TiO_2$  porous nanorods with a low refractive index (1.38) and a  $TiO_2$  dense layer with a high refractive index (2.45) was presented by Khan et al. according to the glancing angle deposition technique [119]. The refractive index of  $TiO_2$  can be tuned from 2.4 to 1.38 at 550 nm via an oblique angle (Figure 18). The coating exhibited good mechanical resistance, high transparency, and good AR properties on several substrates. Nano-texture enhanced the photocatalytic properties for self-cleaning and organic degradation. On the downside, the coating was not durable. An increase in reflectivity of approximately 2% was observed 14 days after the deposition. In order to improve its mechanical strength and adhesion resilience, the coating was annealed after it was deposited, which means it could not be used on polymer substrates. In addition, scratch tests were performed, but not hardness or modulus measurements. Flexible coatings can also be produced from  $TiO_2$ -based materials. By applying the RF-MS method, Miao et al. [120] fabricated porous and amorphous  $TiO_2$  thin films on flexible polyester and cotton fabric substrates, which showed the high potential for  $TiO_2$  films to be used in smart clothing and wearable devices.

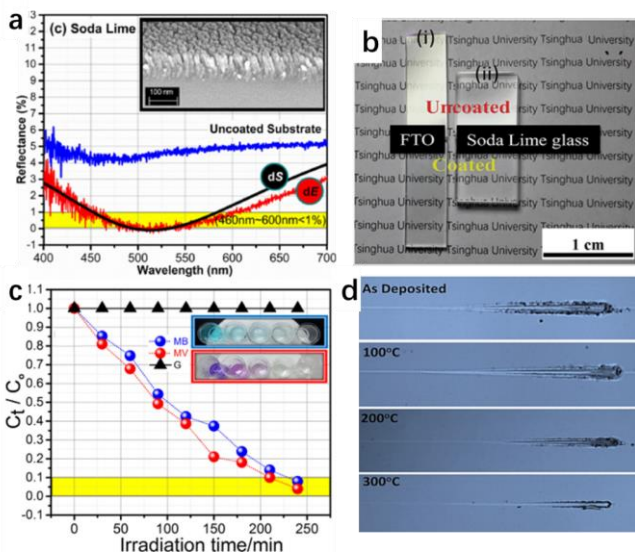


**Figure 18.** (a) Reflectance of TiO<sub>2</sub> coating on soda lime, (b) comparison of coated and uncoated substrates, (c) photocatalytic degradation of MB and MV using TiO<sub>2</sub> coating as a catalyst, (d) optical micrographs of scratches under different annealing temperatures. Reprinted with permission from *Journal of Alloys and Compounds* [119]; Copyright 2020 Elsevier.

Photocatalytic self-cleaning coatings do not require special structures on their surface, which gives them good wear resistance and makes them suitable for MS methods. A variety of materials from a wide variety of sources are inexpensive and suitable for industrial applications. There are many reports of such coatings, and TiO<sub>2</sub> self-cleaning glass is already in commercial use. However, several problems still need to be solved in pursuit of the large-scale application of such coatings. For example, TiO<sub>2</sub> is a wide band-gap (3.2 eV) semiconductor that is active under ultraviolet radiation, which constitutes only 4%–5% of the solar spectrum [116]. The anatase and rutile TiO<sub>2</sub> phases are superior photocatalysts to the amorphous structure [121,122]. However, in order to obtain the anatase or rutile phase, substrate heating or annealing processes are needed [122], which raises the cost of manufacturing TiO<sub>2</sub> coatings and prevents their deposition on polymer substrates. When the deposition temperature is low, the deposited films are generally amorphous [123], which is suitable for transparent applications because of the weak internal scattering. However, the high recombination rate of photo-induced electrons and holes in amorphous TiO<sub>2</sub> further weakens its photocatalytic activity. Elemental doping [124] and coupling TiO<sub>2</sub> with another semiconductor having a different band gap [116,125] are usually used to improve photocatalytic activity. By applying DC-MS and high-power impulse MS (HPIMS), Abidi et al. [125] deposited Cu<sub>x</sub>O/ TiO<sub>2</sub> coating on a polyester cloth to purify volatile organic substances indoors and outdoors according to visible photocatalytic reactions. The low deposition temperatures, high photocatalytic activity and flexibility of Cu<sub>x</sub>O/ TiO<sub>2</sub> coating demonstrates the potential of TiO<sub>2</sub>-based coatings for multifunctional coating applications.

### 5.3 Advances in Multifunctional Coatings in Multilayer Structures

One-component coatings cannot satisfy multifunctional needs. Enhancing overall performance by compounding different materials is a common tool used in the design of materials [50,85,126]. The MS deposition of multilayer coatings is a highly efficient method for the preparation of composite materials for a wide range of applications in tribology [127], optics [128], biomedical [24], and other fields. Multilayer structures are one of the most promising approaches to improving flexibility while maintaining high hardness. For example, an Si/DLC coating prepared by Penkov et al. showed a high hardness of 38–45 GPa, and a H/E ratio of 0.15, which suggests the high flexibility of such a

coating. This coating is deposited at room temperature and thus can be deposited on plastic substrates. However, the coating is not transparent. Later, Penkov et al. [78] prepared  $\text{SiN}_x/\text{BN}$  periodical nanolayered coatings (shown in Figure 19) by MS. In this system,  $\text{SiN}_x$  is hard but semi-transparent. BN is relatively soft and more transparent. The desired balance between hardness, flexibility, and transparency was achieved by combining the different characteristics of  $\text{SiN}_x$  and BN. The thickness of each layer and sputtering condition also contributed to adjusting the coating properties. All the performances make it promising for multifunctional protective coatings. However, this research did not discuss wetting or self-cleaning ability.

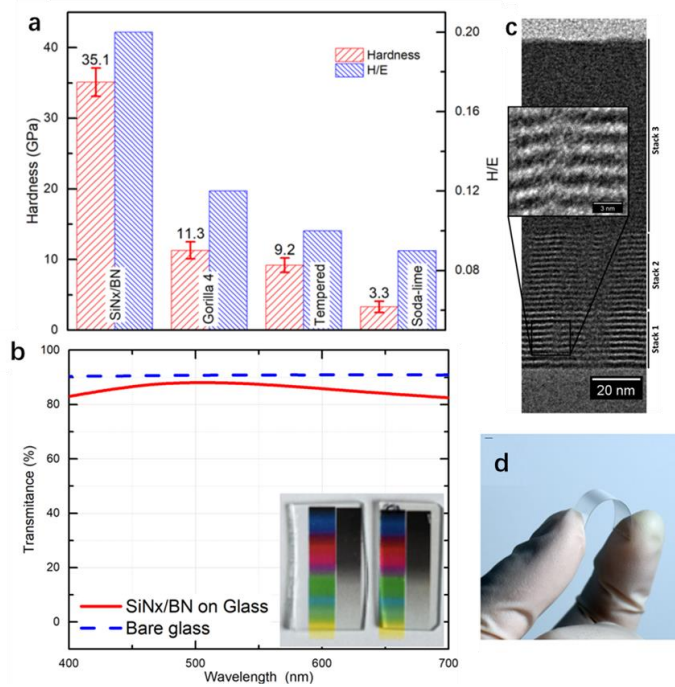


**Figure 19.** (a) and (b), Mechanical and optical properties, (c)TEM image of the cross-section, (d) photo of  $\text{SiN}_x/\text{BN}$  PNCs. Reprinted with permission from *ACS Applied Materials & Interfaces* [78]; Copyright 2019 American Chemical Society.

Mazur et al. [90] presented a functional photocatalytically active and scratch-resistant AR coating based on  $\text{TiO}_2$  and  $\text{SiO}_2$  using microwave-assisted DC-MS. This AR coating consisted of five thin films with high ( $\text{TiO}_2$ ) and low ( $\text{SiO}_2$ ) refractive indexes. Unlike conventional AR coatings, the top layer was  $\text{TiO}_2$  rather than  $\text{SiO}_2$  to impart a self-cleaning capability to the coating. The coating possessed an increased hardness of 9.8 GPa and increased scratch resistance compared with the glass substrate, a high transmittance of 97%, and a low reflectance of approximately 3%. Due to the thin  $\text{TiO}_2$  top layer (just 10 nm) of the coating, it had a photocatalytic effect: after 12 h of UV-vis exposure, the deposited coating decomposed almost 30% of phenol. The results are shown in Figure 20. It is worth noting that the coating in this study exhibited intrinsic hydrophobicity with a CA of 91.1°. However, the authors did not test its photo-induced hydrophilicity or intuitive self-cleaning performance.

Reports on using MS technology to produce flexible hard coatings that are also transparent and self-cleaning are still rare. There are numerous reports on multilayer coatings, and significant efforts have been made to enhance their desired functions. The  $\text{SiN}_x/\text{BN}$  periodical nano-multilayer coating presented by Penkov et al. may be a good example of a flexible, multifunctional coating prepared by MS technology. Along this line, more efficient multifunctional coatings could be designed using periodical multilayer structures.

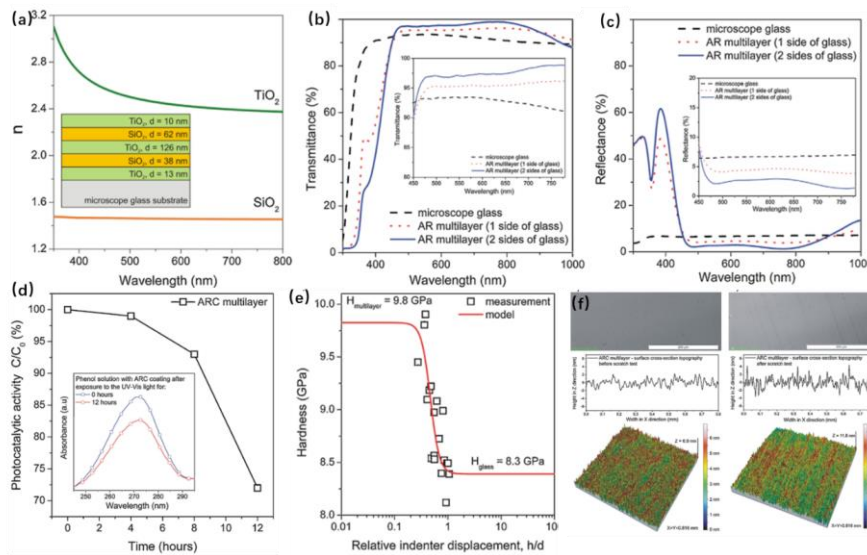


**Figure 20.** (a) Structure of AR coating and refractive index of  $\text{TiO}_2$  and  $\text{SiO}_2$ . (b) and (d) Transmittance and reflectance of AR coating. (d) Photocatalytic activity. (e) Hardness and (f) optical microscopy profilometry investigations before (left) and after (right) scratch test. Reprinted with permission from *Applied Surface Science* [90]; Copyright 2016 Elsevier.

## 6. Conclusions and Outlook

Self-cleaning coatings with high hardness, flexibility, transparency, antireflection, and self-cleaning properties are strongly needed in modern society. The trade-offs between the different properties that are desired are hindering their application. Understanding and attempting to balance these trade-offs are essential to promoting the development of multifunctional coatings. This review summarises the basic principles of wetting ability, other properties required for multifunctional self-cleaning coatings, testing methods, and common means of coating preparation.

Though many efforts have been made to improve the comprehensive performance of multifunctional coatings, numerous problems still have not been solved. Mechanical properties, including high hardness and durability, are the most important issues, especially for polymer coatings, as these have been the most-studied coatings to date. We highlight the current research status of MS technology in multifunctional coating preparation, as MS can easily produce the desired mechanical and optical properties. Moreover, it is one of the most commonly used coating technologies today. However, more research is needed. Multilayer coatings deposited by MS technology combine the properties of different materials that are already widely used for wear resistance, high hardness, and optics. Recent research has demonstrated the great potential of such structures in the preparation of coatings with high hardness, flexibility, and transparency. Nevertheless, further research is still needed to provide them with self-cleaning properties.

Photocatalytic materials represented by  $\text{TiO}_2$  have good mechanical and optical properties.  $\text{TiO}_2$ -based self-cleaning and AR coatings on glass deposited by MS have been extensively researched. However, most of the research should have mentioned the mechanical properties of such coatings. A few studies have shown the high hardness of  $\text{TiO}_2$  and the low temperatures at which it can be deposited on flexible substrates using MS. These results suggest the possibility of multifunctional coatings with improved properties made from  $\text{TiO}_2$ . The preparation of multilayer coatings from materials such as  $\text{TiO}_2$  merits further research.

**Funding:** This research received no external funding.

**Acknowledgments:** This work was supported by the Zhejiang University/University of Illinois at Urbana-Champaign Institute.

**Conflicts of Interest:** The authors declare no conflict of interest.

## References

1. Lin, X.; Li, H.-T.; Nie, M.-X.; Fu, S.-R.; Li, Y.; Zhang, Q.; Chen, F.; Han, D.; Fu, Q. Engineering the Properties of Transparent Hybrid Coating toward High Hardness, Excellent Flexibility, and Multifunction. *ACS Appl. Mater. Interfaces* **2022**, *14*, 39432–39440, doi:10.1021/acsami.2c13256.
2. Dalawai, S.P.; Saad Aly, M.A.; Latthe, S.S.; Xing, R.; Sutar, R.S.; Nagappan, S.; Ha, C.-S.; Kumar Sadasivuni, K.; Liu, S. Recent Advances in Durability of Superhydrophobic Self-Cleaning Technology: A Critical Review. *Prog. Org. Coat.* **2020**, *138*, 105381, doi:10.1016/j.porgcoat.2019.105381.
3. Bai, Y.; Zhang, H.; Shao, Y.; Zhang, H.; Zhu, J. Recent Progresses of Superhydrophobic Coatings in Different Application Fields: An Overview. *Coatings* **2021**, *11*, 116, doi:10.3390/coatings11020116.
4. Guo, H.; Xu, T.; Zhang, J.; Zhao, W.; Zhang, J.; Lin, C.; Zhang, L. A Multifunctional Anti-Fog, Antibacterial, and Self-Cleaning Surface Coating Based on Poly(NVP-Co-MA). *Chem. Eng. J.* **2018**, *351*, 409–417, doi:10.1016/j.cej.2018.06.062.
5. Howarter, J.A.; Youngblood, J.P. Self-Cleaning and Anti-Fog Surfaces via Stimuli-Responsive Polymer Brushes. *Adv. Mater.* **2007**, *19*, 3838–3843, doi:10.1002/adma.200700156.
6. Parkin, I.P.; Palgrave, R.G. Self-Cleaning Coatings. *J. Mater. Chem.* **2005**, *15*, 1689, doi:10.1039/b412803f.
7. Ellinas, K.; Tserepi, A.; Gogolides, E. Durable Superhydrophobic and Superamphiphobic Polymeric Surfaces and Their Applications: A Review. *Adv. Colloid Interface Sci.* **2017**, *250*, 132–157, doi:10.1016/j.cis.2017.09.003.
8. Mortazavi, V.; Khonsari, M.M. On the Degradation of Superhydrophobic Surfaces: A Review. *Wear* **2017**, *372–373*, 145–157, doi:10.1016/j.wear.2016.11.009.
9. Ritchie, R.O. The Conflicts between Strength and Toughness. *Nat. Mater.* **2011**, *10*, 817–822, doi:10.1038/nmat3115.
10. Garner, S.; Glaesemann, S.; Li, X. Ultra-Slim Flexible Glass for Roll-to-Roll Electronic Device Fabrication. *Appl. Phys. A* **2014**, *116*, 403–407, doi:10.1007/s00339-014-8468-2.
11. Auch, M.D.J.; Soo, O.K.; Ewald, G.; Soo-Jin, C. Ultrathin Glass for Flexible OLED Application. *Thin Solid Films* **2002**, *417*, 47–50, doi:10.1016/S0040-6090(02)00647-8.
12. Demetriou, M.D.; Launey, M.E.; Garrett, G.; Schramm, J.P.; Hofmann, D.C.; Johnson, W.L.; Ritchie, R.O. A Damage-Tolerant Glass. *Nat. Mater.* **2011**, *10*, 123–128, doi:10.1038/nmat2930.
13. Lee, Y.; Lee, H.; Im, H.-G.; Jo, W.; Choi, G.-M.; Kim, T.-S.; Jang, J.; Bae, B.-S. Transparent and Flexible Hybrid Cover Window Film: Hard Coating/Substrate All-in-One Composite Film for Reliable Foldable Display. *Compos. Part B Eng.* **2022**, *247*, 110336, doi:10.1016/j.compositesb.2022.110336.
14. Kumar, D.; Wu, X.; Fu, Q.; Ho, J.W.C.; Kanhere, P.D.; Li, L.; Chen, Z. Hydrophobic Sol–Gel Coatings Based on Polydimethylsiloxane for Self-Cleaning Applications. *Mater. Des.* **2015**, *86*, 855–862, doi:10.1016/j.matdes.2015.07.174.
15. Chen, R.; Xie, Q.; Zeng, H.; Ma, C.; Zhang, G. Non-Elastic Glassy Coating with Fouling Release and Resistance Abilities. *J. Mater. Chem. A* **2020**, *8*, 380–387, doi:10.1039/C9TA09794E.
16. Bae, G.; Choi, G.-M.; Ahn, C.; Kim, S.-M.; Kim, W.; Choi, Y.; Park, D.; Jang, D.; Hong, J.-W.; Han, S.M.; et al. Flexible Protective Film: Ultrahard, Yet Flexible Hybrid Nanocomposite Reinforced by 3D Inorganic Nanoshell Structures. *Adv. Funct. Mater.* **2021**, *31*, 2010254, doi:10.1002/adfm.202010254.
17. Xu, C.-L.; Song, F.; Wang, X.-L.; Wang, Y.-Z. Surface Modification with Hierarchical CuO Arrays toward a Flexible, Durable Superhydrophobic and Self-Cleaning Material. *Chem. Eng. J.* **2017**, *313*, 1328–1334, doi:10.1016/j.cej.2016.11.024.

18. Kumar, D.; Li, L.; Chen, Z. Mechanically Robust Polyvinylidene Fluoride (PVDF) Based Superhydrophobic Coatings for Self-Cleaning Applications. *Prog. Org. Coat.* **2016**, *101*, 385–390, doi:10.1016/j.porgcoat.2016.09.003.

19. Chen, X.; Wang, M.; Xin, Y.; Huang, Y. One-Step Fabrication of Self-Cleaning Superhydrophobic Surfaces: A Combined Experimental and Molecular Dynamics Study. *Surf. Interfaces* **2022**, *31*, 102022, doi:10.1016/j.surfin.2022.102022.

20. Jiang, L.; Hou, P.; He, S.; Han, M.; Xiang, P.; Xiao, T.; Tan, X. The Robust Superhydrophobic SiO<sub>2</sub>/Diatomite/PDMS/KH-570/Me-MQ Composite Coating for Self-Cleaning Application of Building Surface. *Colloids Surf. Physicochem. Eng. Asp.* **2022**, *634*, 127936, doi:10.1016/j.colsurfa.2021.127936.

21. Cully, P.; Karasu, F.; Müller, L.; Jauzein, T.; Leterrier, Y. Self-Cleaning and Wear-Resistant Polymer Nanocomposite Surfaces. *Surf. Coat. Technol.* **2018**, *348*, 111–120, doi:10.1016/j.surfcoat.2018.05.040.

22. Deng, W.; Long, M.; Miao, X.; Wen, N.; Deng, W. Eco-Friendly Preparation of Robust Superhydrophobic Cu(OH)<sub>2</sub> Coating for Self-Cleaning, Oil-Water Separation and Oil Sorption. *Surf. Coat. Technol.* **2017**, *325*, 14–21, doi:10.1016/j.surfcoat.2017.06.040.

23. Krella, A. Resistance of PVD Coatings to Erosive and Wear Processes: A Review. *Coatings* **2020**, *10*, 921, doi:10.3390/coatings10100921.

24. Penkov, O.V.; Khadem, M.; Lee, J.-S.; Kheradmandfar, M.; Kim, C.-L.; Cho, S.-W.; Kim, D.-E. Highly Durable and Biocompatible Periodical Si/DLC Nanocomposite Coatings. *Nanoscale* **2018**, *10*, 4852–4860, doi:10.1039/C7NR06762C.

25. Gilewicz, A.; Warcholinski, B.; Szymanski, W.; Grimm, W. CrCN/CrN+ta-C Multilayer Coating for Applications in Wood Processing. *Tribol. Int.* **2013**, *57*, 1–7, doi:10.1016/j.triboint.2012.07.006.

26. Čolović, B.; Kisić, D.; Jokanović, B.; Rakočević, Z.; Nasov, I.; Petkoska, A.T.; Jokanović, V. Wetting Properties of Titanium Oxides, Oxynitrides and Nitrides Obtained by DC and Pulsed Magnetron Sputtering and Cathodic Arc Evaporation. *Mater. Sci.-Pol.* **2019**, *37*, 173–181, doi:10.2478/msp-2019-0031.

27. Dobromir, M.; Apetrei, R.P.; Rebegea, S.; Manole, A.V.; Nica, V.; Luca, D. Synthesis and Characterization of RF Sputtered WO<sub>3</sub>/TiO<sub>2</sub> Bilayers. *Surf. Coat. Technol.* **2016**, *285*, 197–202, doi:10.1016/j.surfcoat.2015.11.031.

28. Liu, Y.Y.; Qian, L.Q.; Guo, C.; Jia, X.; Wang, J.W.; Tang, W.H. Natural Superhydrophilic TiO<sub>2</sub>/SiO<sub>2</sub> Composite Thin Films Deposited by Radio Frequency Magnetron Sputtering. *J. Alloys Compd.* **2009**, *479*, 532–535, doi:10.1016/j.jallcom.2008.12.125.

29. Zhang, C.; Peng, Z.; Cui, X.; Neil, E.; Li, Y.; Kasap, S.; Yang, Q. Reversible Superhydrophilicity and Hydrophobicity Switching of V<sub>2</sub>O<sub>5</sub> Thin Films Deposited by Magnetron Sputtering. *Appl. Surf. Sci.* **2018**, *433*, 1094–1099, doi:10.1016/j.apsusc.2017.10.146.

30. Gao, W.; Ma, F.; Yin, Y.; Li, J. Robust and Durable Transparent Superhydrophobic F-TNTs/TiN Coating Fabricated by Structure Tuning on Surface of TiN Hard Coating. *Appl. Surf. Sci.* **2023**, *613*, 155967, doi:10.1016/j.apsusc.2022.155967.

31. Kratochvíl, J.; Kuzminova, A.; Solař, P.; Hanuš, J.; Kylián, O.; Biederman, H. Wetting and Drying on Gradient-Nanostructured C:F Surfaces Synthesized Using a Gas Aggregation Source of Nanoparticles Combined with Magnetron Sputtering of Polytetrafluoroethylene. *Vacuum* **2019**, *166*, 50–56, doi:10.1016/j.vacuum.2019.04.050.

32. Yuan, Y.; Duan, Y.; Zuo, Z.; Yang, L.; Liao, R. Novel, Stable and Durable Superhydrophobic Film on Glass Prepared by RF Magnetron Sputtering. *Mater. Lett.* **2017**, *199*, 97–100, doi:10.1016/j.matlet.2017.04.067.

33. Luo, B.; Deng, Y.; Wang, Y.; Shi, Y.; Cao, L.; Zhu, W. Magnetron Sputtering Based Direct Fabrication of Three Dimensional CdTe Hierarchical Nanotrees Exhibiting Stable Superhydrophobic Property. *Appl. Surf. Sci.* **2013**, *280*, 550–555, doi:10.1016/j.apsusc.2013.05.025.

34. Veziroglu, S.; Röder, K.; Gronenberg, O.; Vahl, A.; Polonskyi, O.; Strunskus, T.; Rubahn, H.-G.; Kienle, L.; Adam, J.; Fiutowski, J.; et al. Cauliflower-like  $\text{CeO}_2$ – $\text{TiO}_2$  Hybrid Nanostructures with Extreme Photocatalytic and Self-Cleaning Properties. *Nanoscale* **2019**, *11*, 9840–9844, doi:10.1039/C9NR01208G.

35. Xin, L.; Li, H.; Gao, J.; Wang, Z.; Zhou, K.; Yu, S. Large-Scale Fabrication of Decoupling Coatings with Promising Robustness and Superhydrophobicity for Antifouling, Drag Reduction, and Organic Photodegradation. *Friction* **2023**, *11*, 716–736, doi:10.1007/s40544-022-0652-3.

36. Khadem, M.; Penkov, O.V.; Yang, H.-K.; Kim, D.-E. Tribology of Multilayer Coatings for Wear Reduction: A Review. *Friction* **2017**, *5*, 248–262, doi:10.1007/s40544-017-0181-7.

37. Extremely Durable Biofouling-Resistant Metallic Surfaces Based on Electrodeposited Nanoporous Tungstite Films on Steel | Nature Communications Available online: <https://www.nature.com/articles/ncomms9649> (accessed on 19 March 2023).

38. Li, G.-X.; Liu, Y.; Wang, B.; Song, X.-M.; Li, E.; Yan, H. Preparation of Transparent BN Films with Superhydrophobic Surface. *Appl. Surf. Sci.* **2008**, *254*, 5299–5303, doi:10.1016/j.apsusc.2008.01.170.

39. Sambasivam, S.; Maram, P.S.; Muralee Gopi, C.V.V.; Obaidat, I.M. Effect of Erbium on the Structural, Morphological, and Optical Properties of  $\text{SnO}_2$  Thin Films Deposited by Spray Pyrolysis. *Optik* **2020**, *202*, 163596, doi:10.1016/j.jleo.2019.163596.

40. Wu, Y.; Du, J.; Liu, G.; Ma, D.; Jia, F.; Klemeš, J.J.; Wang, J. A Review of Self-Cleaning Technology to Reduce Dust and Ice Accumulation in Photovoltaic Power Generation Using Superhydrophobic Coating. *Renew. Energy* **2022**, *185*, 1034–1061, doi:10.1016/j.renene.2021.12.123.

41. Bao, Y.; Chang, J.; Zhang, Y.; Chen, L. Robust Superhydrophobic Coating with Hollow  $\text{SiO}_2$ /PAA-b-PS Janus Microspheres for Self-Cleaning and Oil-Water Separation. *Chem. Eng. J.* **2022**, *446*, 136959, doi:10.1016/j.cej.2022.136959.

42. Xiao, S.; Hao, X.; Yang, Y.; Li, L.; He, N.; Li, H. Feasible Fabrication of a Wear-Resistant Hydrophobic Surface. *Appl. Surf. Sci.* **2019**, *463*, 923–930, doi:10.1016/j.apsusc.2018.09.030.

43. Young, T. III. An Essay on the Cohesion of Fluids. *Philos. Trans. R. Soc. Lond.* **1997**, *95*, 65–87, doi:10.1098/rstl.1805.0005.

44. Zhang, D.; Wang, L.; Qian, H.; Li, X. Superhydrophobic Surfaces for Corrosion Protection: A Review of Recent Progresses and Future Directions. *J. Coat. Technol. Res.* **2016**, *13*, 11–29, doi:10.1007/s11998-015-9744-6.

45. Cassie, A.B.D.; Baxter, S. Wettability of Porous Surfaces. *Trans. Faraday Soc.* **1944**, *40*, 546, doi:10.1039/tf9444000546.

46. Yao, L.; He, J. Recent Progress in Antireflection and Self-Cleaning Technology – From Surface Engineering to Functional Surfaces. *Prog. Mater. Sci.* **2014**, *61*, 94–143, doi:10.1016/j.pmatsci.2013.12.003.

47. Zhao, J.; Gao, X.; Chen, S.; Lin, H.; Li, Z.; Lin, X. Hydrophobic or Superhydrophobic Modification of Cement-Based Materials: A Systematic Review. *Compos. Part B Eng.* **2022**, *243*, 110104, doi:10.1016/j.compositesb.2022.110104.

48. Niu, W.; Chen, G.Y.; Xu, H.; Liu, X.; Sun, J. Highly Transparent and Self-Healable Solar Thermal Anti-/Deicing Surfaces: When Ultrathin MXene Multilayers Marry a Solid Slippery Self-Cleaning Coating. *Adv. Mater.* **2022**, *34*, 2108232, doi:10.1002/adma.202108232.

49. Garlisi, C.; Trepcı, E.; Li, X.; Al Sakkaf, R.; Al-Ali, K.; Nogueira, R.P.; Zheng, L.; Azar, E.; Palmisano, G. Multilayer Thin Film Structures for Multifunctional Glass: Self-Cleaning, Antireflective and Energy-Saving Properties. *Appl. Energy* **2020**, *264*, 114697, doi:10.1016/j.apenergy.2020.114697.

50. Zhang, Y.; Chen, Z.; Zheng, H.; Chen, R.; Ma, C.; Zhang, G. Multifunctional Hard Yet Flexible Coatings Fabricated Using a Universal Step-by-Step Strategy. *Adv. Sci.* **2022**, *9*, 2200268, doi:10.1002/advs.202200268.

51. Li, X.-M.; Reinhoudt, D.; Crego-Calama, M. What Do We Need for a Superhydrophobic Surface? A Review on the Recent Progress in the Preparation of Superhydrophobic Surfaces. *Chem. Soc. Rev.* **2007**, *36*, 1350–1368, doi:10.1039/B602486F.

52. Zhang, L.; Uzoma, P.C.; Xiaoyang, C.; Penkov, O.V.; Hu, H. Bio-Inspired Hierarchical Micro/Nanostructured Surfaces for Superhydrophobic and Anti-Ice Applications. *Front. Bioeng. Biotechnol.* **2022**, *10*, 872268, doi:10.3389/fbioe.2022.872268.

53. Verho, T.; Bower, C.; Andrew, P.; Franssila, S.; Ikkala, O.; Ras, R.H.A. Mechanically Durable Superhydrophobic Surfaces. *Adv. Mater.* **2011**, *23*, 673–678, doi:10.1002/adma.201003129.

54. Xiu, Y.; Xiao, F.; Hess, D.W.; Wong, C.P. Superhydrophobic Optically Transparent Silica Films Formed with a Eutectic Liquid. *Thin Solid Films* **2009**, *517*, 1610–1615, doi:10.1016/j.tsf.2008.09.081.

55. Zhu, D.; Tan, X.; Ji, L.; Shi, Z.; Zhang, X. Preparation of Transparent and Hydrophobic Cerium Oxide Films with Stable Mechanical Properties by Magnetron Sputtering. *Vacuum* **2021**, *184*, 109888, doi:10.1016/j.vacuum.2020.109888.

56. Lee, H.; Lee, Y.; Lee, S.W.; Kang, S.-M.; Kim, Y.H.; Jo, W.; Kim, T.-S.; Jang, J.; Bae, B.-S. Elongation Improvement of Transparent and Flexible Surface Protective Coating Using Polydimethylsiloxane-Anchored Epoxy-Functionalized Siloxane Hybrid Composite for Reliable out-Foldable Displays. *Compos. Part B Eng.* **2021**, *225*, 109313, doi:10.1016/j.compositesb.2021.109313.

57. Maharjan, S.; Liao, K.-S.; Wang, A.J.; Barton, K.; Haldar, A.; Alley, N.J.; Byrne, H.J.; Curran, S.A. Self-Cleaning Hydrophobic Nanocoating on Glass: A Scalable Manufacturing Process. *Mater. Chem. Phys.* **2020**, *239*, 122000, doi:10.1016/j.matchemphys.2019.122000.

58. Zhong, Q.; Macharia, D.K.; Zhong, W.; Liu, Z.; Chen, Z. Synthesis of Hydrophobic W<sub>18</sub>O<sub>49</sub> Nanorods for Constructing UV/NIR-Shielding and Self-Cleaning Film. *Ceram. Int.* **2020**, *46*, 11898–11904, doi:10.1016/j.ceramint.2020.01.226.

59. Sarkin, A.S.; Ekren, N.; Sağlam, Ş. A Review of Anti-Reflection and Self-Cleaning Coatings on Photovoltaic Panels. *Sol. Energy* **2020**, *199*, 63–73, doi:10.1016/j.solener.2020.01.084.

60. Wang, Y.; Gong, X. Special Oleophobic and Hydrophilic Surfaces: Approaches, Mechanisms, and Applications. *J. Mater. Chem. A* **2017**, *5*, 3759–3773, doi:10.1039/C6TA10474F.

61. England, M.W.; Urata, C.; Dunderdale, G.J.; Hozumi, A. Anti-Fogging/Self-Healing Properties of Clay-Containing Transparent Nanocomposite Thin Films. *ACS Appl. Mater. Interfaces* **2016**, *8*, 4318–4322, doi:10.1021/acsami.5b11961.

62. Ratova, M.; Klaysri, R.; Praserthdam, P.; Kelly, P.J. Visible Light Active Photocatalytic C-Doped Titanium Dioxide Films Deposited via Reactive Pulsed DC Magnetron Co-Sputtering: Properties and Photocatalytic Activity. *Vacuum* **2018**, *149*, 214–224, doi:10.1016/j.vacuum.2018.01.003.

63. Zhao, W.; Lu, H. Self-Cleaning Performance of Super-Hydrophilic Coatings for Dust Deposition Reduction on Solar Photovoltaic Cells. *Coatings* **2021**, *11*, 1059, doi:10.3390/coatings11091059.

64. Anandan, S.; Narasinga Rao, T.; Sathish, M.; Rangappa, D.; Honma, I.; Miyauchi, M. Superhydrophilic Graphene-Loaded TiO<sub>2</sub> Thin Film for Self-Cleaning Applications. *ACS Appl. Mater. Interfaces* **2013**, *5*, 207–212, doi:10.1021/am302557z.

65. Banerjee, S.; Dionysiou, D.D.; Pillai, S.C. Self-Cleaning Applications of TiO<sub>2</sub> by Photo-Induced Hydrophilicity and Photocatalysis. *Appl. Catal. B Environ.* **2015**, *176–177*, 396–428, doi:10.1016/j.apcatb.2015.03.058.

66. Wang, R.; Hashimoto, K.; Fujishima, A.; Chikuni, M.; Kojima, E.; Kitamura, A.; Shimohigoshi, M.; Watanabe, T. Light-Induced Amphiphilic Surfaces. *Nature* **1997**, *388*, 431–432, doi:10.1038/41233.

67. Wang, R.; Hashimoto, K.; Fujishima, A.; Chikuni, M.; Kojima, E.; Kitamura, A.; Shimohigoshi, M.; Watanabe, T. Photogeneration of Highly Amphiphilic TiO<sub>2</sub> Surfaces. *Adv. Mater.* **1998**, *10*, 135–138, doi:10.1002/(SICI)1521-4095(199801)10:2<135::AID-ADMA135>3.0.CO;2-M.

68. Su, X.; Li, H.; Lai, X.; Chen, Z.; Zeng, X. Highly Stretchable and Conductive Superhydrophobic Coating for Flexible Electronics. *ACS Appl. Mater. Interfaces* **2018**, *10*, 10587–10597, doi:10.1021/acsami.8b01382.

69. Ge, C.; Cretu, E. A Sacrificial-Layer-Free Fabrication Technology for MEMS Transducer on Flexible Substrate. *Sens. Actuators Phys.* **2019**, *286*, 202–210, doi:10.1016/j.sna.2018.12.049.

70. Musil, J. Flexible Hard Nanocomposite Coatings. *RSC Adv.* **2015**, *5*, 60482–60495, doi:10.1039/C5RA09586G.

71. Zhang, K.; Huang, S.; Wang, J.; Liu, G. Transparent Organic/Silica Nanocomposite Coating That Is Flexible, Omniprophic, and Harder than a 9H Pencil. *Chem. Eng. J.* **2020**, *396*, 125211, doi:10.1016/j.cej.2020.125211.

72. Mehanna, Y.A.; Crick, C.R. Image Analysis Methodology for a Quantitative Evaluation of Coating Abrasion Resistance. *Appl. Mater. Today* **2021**, *25*, 101203, doi:10.1016/j.apmt.2021.101203.

73. Amazon.Com: MXBAOHENG QTX Paint Film Flexibility Tester Elastic Film Tester GB GB/T1731-93 : Tools & Home Improvement Available online: [https://www.amazon.com/-/zh\\_TW/HQ-1317/dp/B077FX74VG](https://www.amazon.com/-/zh_TW/HQ-1317/dp/B077FX74VG) (accessed on 19 May 2023).

74. Yanagisawa, T.; Nakajima, A.; Sakai, M.; Kameshima, Y.; Okada, K. Preparation and Abrasion Resistance of Transparent Super-Hydrophobic Coating by Combining Crater-like Silica Films with Acicular Boehmite Powder. *Mater. Sci. Eng. B* **2009**, *161*, 36–39, doi:10.1016/j.mseb.2008.11.016.

75. Zhang, X.; Liu, S.; Salim, A.; Seeger, S. Hierarchical Structured Multifunctional Self-Cleaning Material with Durable Superhydrophobicity and Photocatalytic Functionalities. *Small* **2019**, *15*, 1901822, doi:10.1002/smll.201901822.

76. Kustandi, T.S.; Loh, W.W.; Shen, L.; Low, H.Y. Reversible Recovery of Nanoimprinted Polymer Structures. *Langmuir* **2013**, *29*, 10498–10504, doi:10.1021/la401621j.

77. Ionov, L.; Synytska, A. Self-Healing Superhydrophobic Materials. *Phys. Chem. Chem. Phys.* **2012**, *14*, 10497–10502, doi:10.1039/C2CP41377A.

78. Penkov, O.V.; Khadem, M.; Kim, D.-E. Hard, Flexible, and Transparent Nanolayered SiNx/BN Periodical Coatings. *ACS Appl. Mater. Interfaces* **2019**, *11*, 9685–9690, doi:10.1021/acsami.8b22091.

79. Wang, M.; Yang, Z.; Yang, C.; Zhang, D.; Tian, Y.; Liu, X. The Investigation of Mechanical and Thermal Properties of Super-Hydrophobic Nitinol Surfaces Fabricated by Hybrid Methods of Laser Irradiation and Carbon Ion Implantation. *Appl. Surf. Sci.* **2020**, *527*, 146889, doi:10.1016/j.apsusc.2020.146889.

80. Zhang, P.; Zhang, G.; Pan, J.; Ma, C.; Zhang, G. Non-Isocyanate Polyurethane Coating with High Hardness, Superior Flexibility, and Strong Substrate Adhesion. *ACS Appl. Mater. Interfaces* **2023**, *15*, 5998–6004, doi:10.1021/acsami.2c22433.

81. Sun, Y.; Singh Rawat, R.; Chen, Z. Mechanically Robust Multifunctional Antifogging Coating on Transparent Plastic Substrates. *Appl. Surf. Sci.* **2022**, *580*, 152307, doi:10.1016/j.apsusc.2021.152307.

82. Zhang, J.; Singh, V.; Huang, W.; Mandal, P.; Tiwari, M.K. Self-Healing, Robust, Liquid-Repellent Coatings Exploiting the Donor–Acceptor Self-Assembly. *ACS Appl. Mater. Interfaces* **2023**, *15*, 8699–8708, doi:10.1021/acsami.2c20636.

83. Hanson, B.; Hofmann, J.; Pasquinelli, M.A. Influence of Copolyester Composition on Adhesion to Soda-Lime Glass via Molecular Dynamics Simulations. *ACS Appl. Mater. Interfaces* **2016**, *8*, 13583–13589, doi:10.1021/acsami.6b01851.

84. Rezaee, M.; Tsai, L.-C.; Haider, M.I.; Yazdi, A.; Sanatizadeh, E.; Salowitz, N.P. Quantitative Peel Test for Thin Films/Layers Based on a Coupled Parametric and Statistical Study. *Sci. Rep.* **2019**, *9*, 19805, doi:10.1038/s41598-019-55355-9.

85. Cheng, W.; Ren, H.; Chen, Y.; Wu, D.; Li, X.; Yu, C.; Li, F. Fabrication of Cu/Cu<sub>2</sub>O/CuO@WO<sub>3</sub> Composite Films with Antireflective, Hydrophilic, and Photocatalytic Properties by Magnetron Sputtering. *Appl. Surf. Sci.* **2022**, *585*, 152714, doi:10.1016/j.apsusc.2022.152714.

86. Motamedi, M.; Warkiani, M.E.; Taylor, R.A. Transparent Surfaces Inspired by Nature. *Adv. Opt. Mater.* **2018**, *6*, 1800091, doi:10.1002/adom.201800091.

87. Cai, J.; Qi, L. Recent Advances in Antireflective Surfaces Based on Nanostructure Arrays. *Mater. Horiz.* **2014**, *2*, 37–53, doi:10.1039/C4MH00140K.

88. Schulz, U. Review of Modern Techniques to Generate Antireflective Properties on Thermoplastic Polymers. *Appl. Opt.* **2006**, *45*, 1608–1618, doi:10.1364/AO.45.001608.

89. Ruud, C.J.; Cleri, A.; Maria, J.-P.; Giebink, N.C. Ultralow Index SiO<sub>2</sub> Antireflection Coatings Produced via Magnetron Sputtering. *Nano Lett.* **2022**, *22*, 7358–7362, doi:10.1021/acs.nanolett.2c01945.

90. Mazur, M.; Wojcieszak, D.; Kaczmarek, D.; Domaradzki, J.; Song, S.; Gibson, D.; Placido, F.; Mazur, P.; Kalisz, M.; Poniedzialek, A. Functional Photocatalytically Active and Scratch Resistant Antireflective Coating Based on TiO<sub>2</sub> and SiO<sub>2</sub>. *Appl. Surf. Sci.* **2016**, *380*, 165–171, doi:10.1016/j.apsusc.2016.01.226.

91. Kumar, D.; Wu, X.; Fu, Q.; Ho, J.W.C.; Kanhere, P.D.; Li, L.; Chen, Z. Development of Durable Self-Cleaning Coatings Using Organic–Inorganic Hybrid Sol–Gel Method. *Appl. Surf. Sci.* **2015**, *344*, 205–212, doi:10.1016/j.apsusc.2015.03.105.

92. Huang, Z.; Li, Z.; Zhang, X.; Zhang, Z.; Chen, J. (0 0 1) Facets Optimized Surface Oxygen Vacancies in TiO<sub>2</sub> Films to Enhance Photocatalytic Antibacterial and Hydrophilic Properties. *Appl. Surf. Sci.* **2023**, *616*, 156571, doi:10.1016/j.apsusc.2023.156571.

93. Zuo, Z.; Gao, J.; Liao, R.; Zhao, X.; Yuan, Y. A Novel and Facile Way to Fabricate Transparent Superhydrophobic Film on Glass with Self-Cleaning and Stability. *Mater. Lett.* **2019**, *239*, 48–51, doi:10.1016/j.matlet.2018.12.059.

94. Xu, Z.; Guo, Y.; Liu, Y.; Jia, B.; Sha, P.; Li, L.; Yu, Z.; Zhang, Z.; Ren, L. An Extremely Efficiency Method to Achieve Stable Superhydrophobicity on the Surface of Additive Manufactured NiTi Alloys: “Ultrasonic Fluorination.” *Appl. Surf. Sci.* **2023**, *612*, 155947, doi:10.1016/j.apsusc.2022.155947.

95. and, B.Q.; Shen\*, Z. Fabrication of Superhydrophobic Surfaces by Dislocation-Selective Chemical Etching on Aluminum, Copper, and Zinc Substrates Available online: <https://pubs.acs.org/doi/full/10.1021/la051308c> (accessed on 12 May 2023).

96. Balu, B.; Breedveld, V.; Hess, D.W. Fabrication of “Roll-off” and “Sticky” Superhydrophobic Cellulose Surfaces via Plasma Processing. *Langmuir* **2008**, *24*, 4785–4790, doi:10.1021/la703766c.

97. Fresno, F.; González, M.U.; Martínez, L.; Fernández-Castro, M.; Barawi, M.; Villar-García, I.J.; Soler-Morala, J.; Reñones, P.; Luna, M.; Huttel, Y.; et al. Photo-Induced Self-Cleaning and Wettability in TiO<sub>2</sub> Nanocolumn Arrays Obtained by Glancing-Angle Deposition with Sputtering. *Adv. Sustain. Syst.* **2021**, *5*, 2100071, doi:10.1002/adsu.202100071.

98. Lukong, V.T.; Ukoba, K.; Jen, T.-C. Review of Self-Cleaning TiO<sub>2</sub> Thin Films Deposited with Spin Coating. *Int. J. Adv. Manuf. Technol.* **2022**, *122*, 3525–3546, doi:10.1007/s00170-022-10043-3.

99. Wu, Y.; Tan, X.; Wang, Y.; Tao, F.; Yu, M.; Chen, X. Nonfluorinated, Transparent, and Antireflective Hydrophobic Coating with Self-Cleaning Function. *Colloids Surf. Physicochem. Eng. Asp.* **2022**, *634*, 127919, doi:10.1016/j.colsurfa.2021.127919.

100. Xia, X.; Liu, J.; Liu, Y.; Lei, Z.; Han, Y.; Zheng, Z.; Yin, J. Preparation and Characterization of Biomimetic SiO<sub>2</sub>-TiO<sub>2</sub>-PDMS Composite Hydrophobic Coating with Self-Cleaning Properties for Wall Protection Applications. *Coatings* **2023**, *13*, 224, doi:10.3390/coatings13020224.

101. Seifi, A.; Salari, D.; Khataee, A.; Çoşut, B.; Arslan, L.Ç.; Niaezi, A. Enhanced Photocatalytic Activity of Highly Transparent Superhydrophilic Doped TiO<sub>2</sub> Thin Films for Improving the Self-Cleaning Property of Solar Panel Covers. *Ceram. Int.* **2023**, *49*, 1678–1689, doi:10.1016/j.ceramint.2022.09.130.

102. Ismail, A.A.; Al-Hajji, L.; Azad, I.S.; Al-Yaqoot, A.; Habibi, N.; Alseidi, M.; Ahmed, Sh. Self-Cleaning Application of Mesoporous ZnO, TiO<sub>2</sub> and Fe<sub>2</sub>O<sub>3</sub> Films with the Accommodation of Silver Nanoparticles for Antibacterial Activity. *J. Taiwan Inst. Chem. Eng.* **2023**, *142*, 104627, doi:10.1016/j.jtice.2022.104627.

103. Seifi, A.; Salari, D.; Khataee, A.; Çoşut, B.; Arslan, L.Ç.; Niaezi, A. Enhanced Photocatalytic Activity of Highly Transparent Superhydrophilic Doped TiO<sub>2</sub> Thin Films for Improving the Self-Cleaning Property of Solar Panel Covers. *Ceram. Int.* **2023**, *49*, 1678–1689, doi:10.1016/j.ceramint.2022.09.130.

104. Raut, H.K.; Ganesh, V.A.; Nair, A.S.; Ramakrishna, S. Anti-Reflective Coatings: A Critical, in-Depth Review. *Energy Environ. Sci.* **2011**, *4*, 3779–3804, doi:10.1039/C1EE01297E.

105. Park, S.; Huo, J.; Shin, J.; Heo, K.J.; Kalmoni, J.J.; Sathasivam, S.; Hwang, G.B.; Carmalt, C.J. Production of an EP/PDMS/SA/AlZnO Coated Superhydrophobic Surface through an Aerosol-Assisted Chemical Vapor Deposition Process. *Langmuir* **2022**, *38*, 7825–7832, doi:10.1021/acs.langmuir.2c01060.

106. Mauchauffé, R.; Kang, S.; Moon, S.Y. Fast Formation of Amorphous Titanium Dioxide Thin Films Using a Liquid-Assisted Plasma-Enhanced Deposition Process in Open Air. *Surf. Coat. Technol.* **2019**, *376*, 84–89, doi:10.1016/j.surfcoat.2018.01.088.

107. Weihao, L.; Shengnan, C.; Jianxun, W.; Shaohui, J.; Chenlu, S.; Yong, L.; Gaorong, H. Study on Structural, Optical and Hydrophilic Properties of FTO/TiO<sub>2</sub> Tandem Thin Film Prepared by Aerosol-Assisted Chemical Vapor Deposition Method. *Surf. Coat. Technol.* **2019**, *358*, 715–720, doi:10.1016/j.surfcoat.2018.11.098.

108. Zhang, L.; Xue, C.-H.; Cao, M.; Zhang, M.-M.; Li, M.; Ma, J.-Z. Highly Transparent Fluorine-Free Superhydrophobic Silica Nanotube Coatings. *Chem. Eng. J.* **2017**, *320*, 244–252, doi:10.1016/j.cej.2017.03.048.

109. Tan, X.-Q.; Liu, J.-Y.; Niu, J.-R.; Liu, J.-Y.; Tian, J.-Y. Recent Progress in Magnetron Sputtering Technology Used on Fabrics. *Materials* **2018**, *11*, 1953, doi:10.3390/ma11101953.

110. Yang, M.K. Optical Properties of Teflon® AF Amorphous Fluoropolymers. *J. MicroNanolithography MEMS MOEMS* **2008**, *7*, 033010, doi:10.1117/1.2965541.

111. Sohn, S.; Kim, H.-M.; Jang, J. Super-Hydrophobicity of PTFE Films Coated on an Etched Al Surface by Using a RF-Magnetron Sputtering Method. *J. Korean Phys. Soc.* **2010**, *57*, 1281–1284, doi:10.3938/jkps.57.1281.

112. Tripathi, S.; Haque, S.M.; Rao, K.D.; De, R.; Shripathi, T.; Deshpande, U.; Ganesan, V.; Sahoo, N.K. Investigation of Optical and Microstructural Properties of RF Magnetron Sputtered PTFE Films for Hydrophobic Applications. *Appl. Surf. Sci.* **2016**, *385*, 289–298, doi:10.1016/j.apsusc.2016.05.121.

113. Zenkin, S.; Kos, Š.; Musil, J. Hydrophobicity of Thin Films of Compounds of Low-Electronegativity Metals. *J. Am. Ceram. Soc.* **2014**, *97*, 2713–2717, doi:10.1111/jace.13165.

114. Musil, J.; Zenkin, S.; Kos, Š.; Čerstvý, R.; Haviar, S. Flexible Hydrophobic ZrN Nitride Films. *Vacuum* **2016**, *131*, 34–38, doi:10.1016/j.vacuum.2016.05.020.

115. PalDey, S.; Deevi, S.C. Single Layer and Multilayer Wear Resistant Coatings of (Ti,Al)N: A Review. *Mater. Sci. Eng. A* **2003**, *342*, 58–79, doi:10.1016/S0921-5093(02)00259-9.

116. Karuppasamy, A. Enhanced Photocatalysis and Photohydrophilicity in TiO<sub>2</sub>-W<sub>5</sub>O<sub>14</sub> Nanocomposite Thin Films Grown by in-Lay Sputtering. *Mater. Chem. Phys.* **2023**, *301*, 127580, doi:10.1016/j.matchemphys.2023.127580.

117. Zhao, L.; Zhao, C.; Wang, L.; Fan, X.; Wang, Q.; Liu, J. Preparation and Optical Properties of TiO<sub>2</sub>/SiO<sub>2</sub> Bilayer Antireflection Film. *Opt. Mater.* **2021**, *121*, 111594, doi:10.1016/j.optmat.2021.111594.

118. Lukong, V.T.; Mouchou, R.T.; Enebe, G.C.; Ukoba, K.; Jen, T.C. Deposition and Characterization of Self-Cleaning TiO<sub>2</sub> Thin Films for Photovoltaic Application. *Mater. Today Proc.* **2022**, *62*, S63–S72, doi:10.1016/j.matpr.2022.02.089.

119. Khan, S.B.; Zhang, Z.; Lee, S.L. Single Component: Bilayer TiO<sub>2</sub> as a Durable Antireflective Coating. *J. Alloys Compd.* **2020**, *834*, 155137, doi:10.1016/j.jallcom.2020.155137.

120. Miao, D.; Hu, H.; Li, A.; Jiang, S.; Shang, S. Fabrication of Porous and Amorphous TiO<sub>2</sub> Thin Films on Flexible Textile Substrates. *Ceram. Int.* **2015**, *41*, 9177–9182, doi:10.1016/j.ceramint.2015.03.080.

121. Lelis, M.; Tuckute, S.; Varnagiris, S.; Urbonavicius, M.; Laukaitis, G.; Bockute, K. Tailoring of TiO<sub>2</sub> Film Microstructure by Pulsed-DC and RF Magnetron Co-Sputtering. *Surf. Coat. Technol.* **2019**, *377*, 124906, doi:10.1016/j.surfcoat.2019.124906.

122. Sabbah, H. Effect of Sputtering Parameters on the Self-Cleaning Properties of Amorphous Titanium Dioxide Thin Films. *J. Coat. Technol. Res.* **2017**, *14*, 1423–1433, doi:10.1007/s11998-017-9928-3.

123. Twu, M.J.; Chiou, A.H.; Hu, C.C.; Hsu, C.Y.; Kuo, C.G. Properties of TiO<sub>2</sub> Films Deposited on Flexible Substrates Using Direct Current Magnetron Sputtering and Using High Power Impulse Magnetron Sputtering. *Polym. Degrad. Stab.* **2015**, *117*, 1–7, doi:10.1016/j.polymdegradstab.2015.03.010.

124. Synthesis and Application of Titanium Dioxide Photocatalysis for Energy, Decontamination and Viral Disinfection: A Review | SpringerLink Available online: <https://link.springer.com/article/10.1007/s10311-022-01503-z> (accessed on 12 May 2023).

125. Abidi, M.; Assadi, A.A.; Bouzaza, A.; Hajjaji, A.; Bessais, B.; Rtimi, S. Photocatalytic Indoor/Outdoor Air Treatment and Bacterial Inactivation on Cu<sub>x</sub>O/TiO<sub>2</sub> Prepared by HiPIMS on Polyester Cloth under Low Intensity Visible Light. *Appl. Catal. B Environ.* **2019**, *259*, 118074, doi:10.1016/j.apcatb.2019.118074.

126. Fouad, S.S.; Baradács, E.; Nabil, M.; Parditka, B.; Negm, S.; Erdélyi, Z. Microstructural and Optical Duality of TiO<sub>2</sub>/Cu/TiO<sub>2</sub> Trilayer Films Grown by Atomic Layer Deposition and DC Magnetron Sputtering. *Inorg. Chem. Commun.* **2022**, *145*, 110017, doi:10.1016/j.inoche.2022.110017.

127. Khadem, M.; Penkov, O.V.; Jais, J.; Bae, S.-M.; Dhandapani, V.S.; Kang, B.; Kim, D.-E. Formation of Discrete Periodic Nanolayered Coatings through Tailoring of Nanointerfaces—Toward Zero Macroscale Wear. *Sci. Adv.* **2021**, *7*, eabk1224, doi:10.1126/sciadv.abk1224.

128. Penkov, O.V.; Kopylets, I.A.; Kondratenko, V.V.; Khadem, M. Synthesis and Structural Analysis of Mo/B Periodical Multilayer X-Ray Mirrors for beyond Extreme Ultraviolet Optics. *Mater. Des.* **2021**, *198*, 109318, doi:10.1016/j.matdes.2020.109318.